

MINISTRY OF EDUCATION AND TRAINING

MINISTRY OF CONSTRUCTION

HANOI ARCHITECTURAL UNIVERSITY

=====o O o=====

HOANG HIEU NGHIA

**PLASTIC ANALYSIS OF THE FRAME WITH STEEL
COLUMN AND COMPOSITE STEEL-CONCRETE
BEAM SUPPORT THE STATIC LOAD**

MAJOR: BUILDING AND INDUSTRIAL CONSTRUCTION

CODE: **62 58 02 08**

**ABSTRACT DOCTORAL THESIS
BUILDING AND INDUSTRIAL CONSTRUCTION**

HANOI, 2020

PREAMBLE

1. The urgency of the thesis

In recent years, the research and application and development of steel - concrete composite structures in the world and in Vietnam in the field of structural construction has been interested by researchers and engineers.

When analyzing and calculating structures, they often use traditional design methods, including 2 steps: Step 1: Using linear elastic analysis and the principle of collaboration to determine internal forces and displacements of structural system. Step 2: Check the bearing capacity, stress limits, stability of each individual component.

This traditional design method has been applied for a long time and has the advantage of simplifying the design work of an engineer. However, it does not clearly show the nonlinear relationship between load and displacement, does not clearly show the nonlinearity of the structural material, has not fully considered the behavior of the entire structure so it leads to the material fee. The problem of nonlinear analysis, the force-displacement relationship is nonlinear, must be repeat solved because the structure has been deformed with the previous load and the structural stiffness is weakened, the computer will update the geometric data, material properties after each load change so that it will be close to the actual behavior of the structure. Recently, in the world, when analyzing nonlinear structures, in the standards and researchers often use two basic methods: zone plastic method and plastic hinge method.

The zone plastic method considers the development of the plastic zone slowly as the force exerts on the structure, the plasticity of the elements will be modeled by discrete components of a finite element (divide element bar into n elements) and divide the section into fibers. This method is an accurate way to test other analytical methods, but this method is complex and requires a large analysis time (hundreds of times calculated by the plastic hinge method - according to Ziemian). Therefore it is not suitable for calculating the actual building, only suitable for simple structures, so this method is rarely applied in practice.

The plastic hinge method is a simplified model of the real structure with the assumption that the length of plastic zone $l_h = 0$, whereby it is assumed that during the process of bearing plastic deformation appears and develops only at the two ends of the element, the remaining sections in the bar remain elastic deformation. When conducting plastic analysis, the researchers used the plastic surfaces of Orbison 1982, AISC-LRFD 1994 to consider the yield condition of the cross section, the plastic surfaces has many limitations so it has not been reflected realable behavior of structural systems under load.

Through the above analysis, it can be seen that the problem of constructing the plastic analysis method of the frame structure with steel column and composite beam support the static load for the problem of spreading plasticity analysis of the structural system and the limit load problem of the system the structure, including the spreading plasticity of the composite beam section, the steel column and the plastic deformation zone along the element length and the plastic flow rate of the section, is significant scientific and practical in analyzing the structure and necessary to be researched and applied.

Therefore, the thesis chooses the research topic: "**Plastic analysis of the frame structure with steel column and composite steel-concrete beam support the static load**"

2. Research purposees

i) Building the curve ($M-\phi$) relationship of the composite steel-concrete beam taking into account the plasticity of the material to reflect the actual behavior of the composite beam structure support load; ii) Building the equation of elastic limit surface, intermediate plastic surface, fully plastic surface (failure surface) of the doubly symmetrical wide flange I-

section under axial force combined with biaxial bending moments to predict the bearing capacity of column section steel and builded plastic surface have been applicated into the nonlinear analysis of structural systems; **iii**) Building a finite elements method and computer program applied to nonlinear analysis of the frame structure with steel column and composite steel-concrete beam considers the plasticity of the material and the distributed plasticity of the structural system.

3. Object and scope of researchs

- *Object of research:* Nonlinear analysis of the frame structure with steel column and composite steel-concrete beam support static load considers the plasticity of the material

- *Scope of research:* beam structure, plane frame structure with steel columns and composite steel-concrete beams; model of steel materials regardless of the consolidation period and nonlinear model of tensile and compressive concrete materials; plastic analysis model of the structural system: plastic deformation model spread along the element length; load applied to the structure: static and non-reversible load during the analysis; regardless of the effect of shear deformation in the component; not taking into account the local buckling of the section and the lateral buckling of the component; geometrical nonlinearities are not considered in the analysis process.

4. Research Method

- Using the theoretical research method (analytic method) to develop the nonlinear analysis theory of the frame structure with steel column and composite steel-concrete beam considering the plasticity of the material and the distributed plasticity of the system structure.

- Applying nonlinear decomposition algorithms to build computer programs based on theoretical research results and use to verify the achieved results, in order to accurately and ensure reliability, as well as the feasibility of the results achieved.

5. Scientific and practical significance of the thesis

i) Building the curve ($M-\phi$) relationship of the composite steel-concrete beam taking into account the plasticity of the material to reflect the actual behavior of the composite steel-concrete beam structure support load; **ii**) Building the equation of elastic limit surface, intermediate plastic surface, fully plastic surface (failure surface) of the doubly symmetrical wide flange I-section under axial force combined with biaxial bending moments to predict the bearing capacity of column section steel and builded plastic surface have been applicated into the nonlinear analysis of structural systems; **iii**) Building a finite elements method with plastic multi-point bar elements and computer program applied to nonlinear analysis of the frame structure with steel column and composite steel-concrete beam considers the plasticity of the material and the distributed plasticity of the structural system; **iv**) Building an application computer program for nonlinear analysis of of the frame structure with steel column and composite steel-concrete beam considers the plasticity of the material and the distributed plasticity of the structural system reliably and effectively, apply the program to perform plastic analysis problems.

6. New contributions of the thesis

a) Building the curve ($M-\phi$) relationship of the steel and composite steel-concrete beam to determine the tangent stiffness of these components at different points when the material works in the elastic phase, elastic - plastic and plastic. Establish SPH program to build this relationship.

b) Building the equation of elastic limit surface, intermediate plastic surface, fully plastic surface (failure surface) of the doubly symmetrical wide flange I-section subjected to axial force combined with biaxial bending moments to predict the bearing capacity of section steel column corresponding to a certain design load.

c) Building calculations by finite element method and computer program to analysis the frame structure with steel column and composite steel-concrete beam, taking into account the material nonlinearity when forming multipurpose plasticity points. From this application program, it is possible to determine the limit load factor, plastic flow rate of the section, internal force, displacement of the structure corresponding to different load levels, thereby determining the amount of security full reserve of the structure compared to the design data.

7. The structure of the thesis

The thesis has 4 chapters, introduction, conclusion and appendices

CONTENTS

CHAPTER 1. OVERVIEW OF RESEARCH ISSUES

1.1. Introduction of the frame structure with steel column and composite steel-concrete beam

Studies of composite structures in the world are increasingly being studied more and in many different approaches. In Vietnam, this type of structure has only been studied and applied in the last 10 years and mainly focuses on the study of components and connection calculations, the overall analysis of the structure when the load is low researched, so the approach to studying this type of structure has scientific and practical significance in the construction industry. Within the scope of the thesis, the author has just stopped at studying plane frames with steel columns and composite steel-concrete beams.

1.2. Trends in analysis, design of steel structures and composite structures

Currently, when analyzing and calculating steel structure and composite structure, it is often used traditional methods (Figure 1.1). All three methods of ADS, PD, LRFD require separate inspection of each component, especially taking into account the K factor, not considering the full behavior of the entire structure so that it leads to waste material.

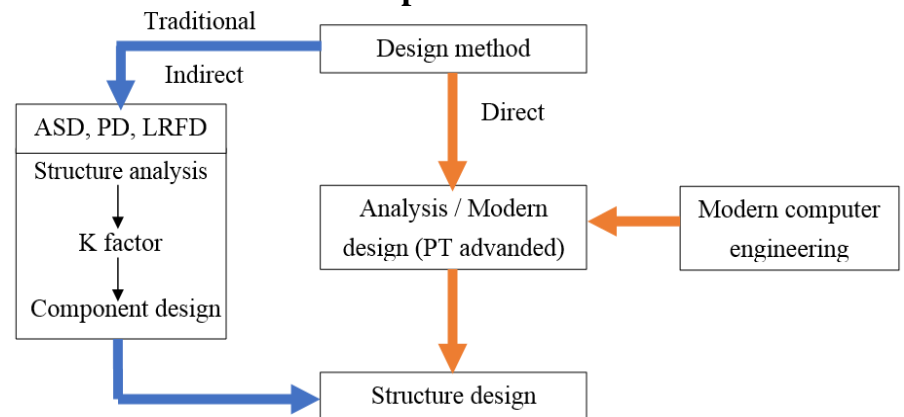


Figure 1.1. structural design and analysis method

Therefore, it is necessary to study modern design (advanced analysis) and only perform in one design step because it will accurately reflect the actual working of the structural system, accurately predict the type of plastic demolition and the limited load of the frame structure under static load and is essential to the reliability of the design.

1.3. Nonlinear analysis and nonlinear analysis levels

1.3.1. Nonlinear analysis

The problem of nonlinear analysis, the force-deformation relationship is a curve, so it must be cyclic solved because the structure has been deformed with the previous load and the structural stiffness is weakened, the computer will update the geometric data, material properties after each load change. The two basic methods used by the researchers when analyzing nonlinear structures are the plastic hinge method and the plastic zone method (Figure 1.2). Some researches on nonlinear materials such as Chan and Chui, White, Wrong, Chen and Sohal, Chen, Kim and Choi, Yong et al, Orbison and Guire, Nguyen Van Tu and Vo Thanh Luong.

1.3.2. Nonlinear analysis levels

In structural analysis, it is difficult to model all nonlinear factors related to structural behavior as in reality in detail. The most common levels of nonlinear analysis are described by the behavioral curves of the static load frame by authors Chan and Chui, Orbison, Nguyen Van Tu, Vu Quoc Anh, Nghiem Manh Hien, Balling and Lyon refers to: first-order elastic analysis, second-order elastic analysis, first-order elastic plastic analysis, second-order elastic plastic analysis.

1.4. Nonlinear model of steel and concrete materials

The thesis used the ideal elastic model according to Eurocode 3 for steel materials, Kent and Park models (1973) for compressible concrete materials, Vebo and Ghali models (1977) for tensile concrete materials.

1.5. Moment – curvature relationship of steel section beam (M-φ)

The process of plastic flow on the section consists of 3 stages: elastic, elastic-plastic and fully plastic (Figure 1.3) ASCE, Michael, Vrouwenvelder.

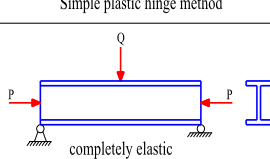
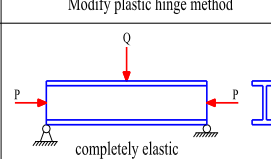
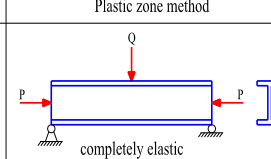
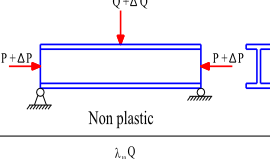
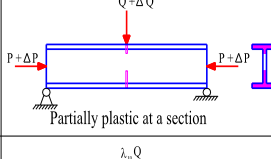
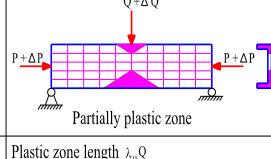
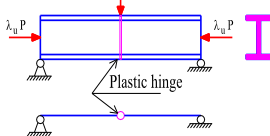
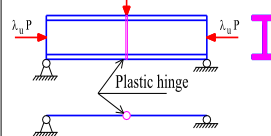
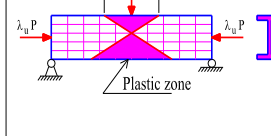
Simple plastic hinge method	Modify plastic hinge method	Plastic zone method
		
		
		

Figure 1.2. Methods of nonlinear material analysis

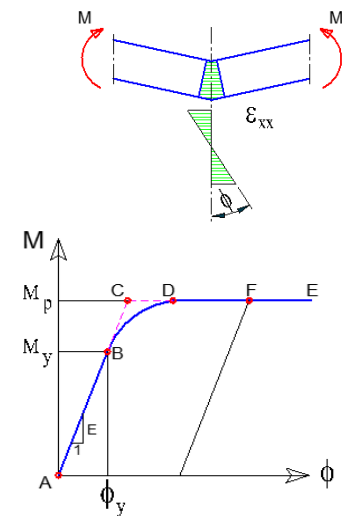


Figure1.3.(M-φ)relationship of section steel beam

1.6. Plastic surface of steel columns

The concept of plastic surface is given to mention the simultaneous effect of axial force and bending moment based on internal force of element. When the bending moment and the axial force in the element reach the yield surface, the plastic hinge is formed. Some typical plastic surface has been proposed and applied with many studies: Orbison, Duan and Chen, AISC-LRFD. This thesis presents the method of constructing the intermediate plastic surface to show the plastic spread across the section in the plastic analysis process of the structure.

1.7. The method of the frame structure analysis when plastic hinge formde

The popular analysis method is the finite element method as shown in Figure 1.4 with many authors used to analyze such as: Chan and Chui, White, Wrong, Chen, Kim and Choi, Orbison and et al, Liew and Chen, Kim and Choi , Cuong and Kim, Doan Ngoc Tinh Nghiem and Ngo Huu Cuong, Abaqus, Ansys, Midas, Adina.

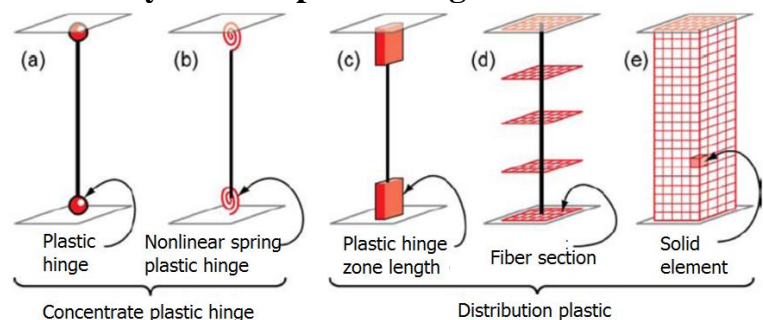


Figure 1.4. beam - column element model in finite element

CHAPTER 2: BUILDING MOMENT – CURVATURE RELATIONSHIP OF STEEL SECTION BEAM AND PLASTIC SURFACE OF STEEL SECTION COLUMN

2.1. Building moment – curvature relationship of steel section beam by the analytical method

The building of moment - curvature relationship of beam section to calculate tangent stiffness at the plastic deformation positions, is the basis for element stiffness and is used in the plastic analysis problem of the structural frame shown in the following chapters. Survey deformation stress diagram of section I steel beam as shown in Figure 2.1.

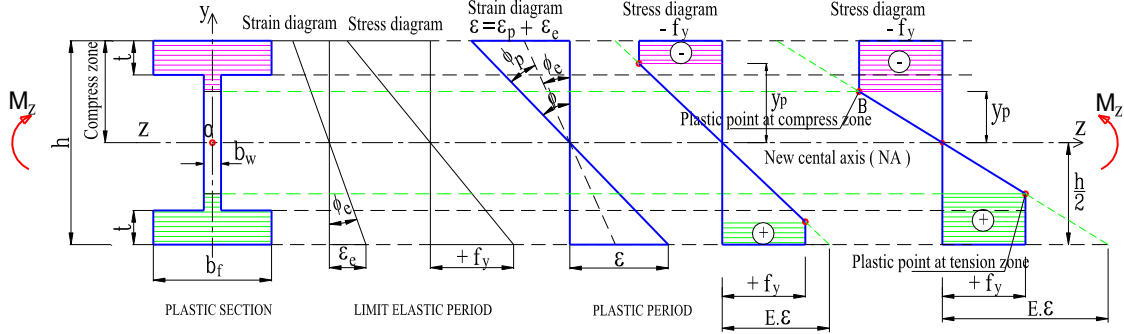


Figure 2.1. Stress and deformation diagram of section I in the main axis z

2.1.1. Plastic moment in main axis (axis z)

- Elastic rotation in axis z: $\phi_{z,e} = 2f_y / hE$ (2.1)

- Elastic moment: $M_{z,e} = 2 \frac{\phi_z E}{3} \left[b_w \left(\frac{h}{2} - t \right)^3 + b_f \left(\left(\frac{h}{2} \right)^3 - \left(\frac{h}{2} - t \right)^3 \right) \right]$ (2.2)

- Elastic limit moment: $M_z = \frac{4 f_y}{3 h} \left[b_w \left(\frac{h}{2} - t \right)^3 + b_f \left(\left(\frac{h}{2} \right)^3 - \left(\frac{h}{2} - t \right)^3 \right) \right]$ (2.3)

- Elastic-plastic moment:

+ Case $\frac{2f_y}{hE} \leq \phi_z \leq \frac{2f_y}{(h-2t)E}$ or $0 \leq \phi_{z,p} \leq \frac{2f_y}{(h-2t)E} - \frac{2f_y}{hE} = \frac{2f_y}{E} \left(\frac{2t}{(h-2t)h} \right)$

$M_z = 2 \left[\frac{\phi_z E b_w}{3} \left(\frac{h}{2} - t \right)^3 + \frac{\phi_z E b_f}{3} \left(\left(\frac{f_y}{\phi_z E} \right)^3 - \left(\frac{h}{2} - t \right)^3 \right) + \frac{f_y b_f}{2} \left(\left(\frac{h}{2} \right)^2 - \left(\frac{f_y}{\phi_z E} \right)^2 \right) \right]$ (2.4)

+ Case $\phi_z > \frac{2f_y}{(h-2t)E}$ or $\phi_{z,p} > \frac{2f_y}{(h-2t)E} - \frac{2f_y}{hE} = \frac{2f_y}{E} \left(\frac{2t}{(h-2t)h} \right)$

$M_z = 2 \left[\frac{f_y b_w}{2} \left(\frac{h}{2} - t \right)^2 - \frac{f_y b_w}{6} \left(\frac{f_y}{\phi_z E} \right)^2 + \frac{f_y b_f t}{2} (h - t) \right]$ (2.5)

- Maximum moment value: $M_{z,max} = 2 \left[\frac{f_y b_w}{2} \left(\frac{h}{2} - t \right)^2 + \frac{f_y b_f t}{2} (h - t) \right]$ (2.6)

2.1.2. Plastic moment in auxiliary axis (axis y)

- Elastic rotation in axis y: $\phi_{y,e} = 2f_y / b_f E$ (2.9)

- Elastic moment: $M_y = [2b_f^3 t + b_w^3 (h - 2t)] \phi_y E / 12$ (2.10)

- Elastic limit moment: $M_{y,e} = [2b_f^3 t + b_w^3 (h - 2t)] f_y / 6b_f$ (2.11)

- Elastic-plastic moment: + Case $\frac{2f_y}{b_f E} \leq \phi_y \leq \frac{2f_y}{b_w E}$ or $0 \leq \phi_{y,p} \leq \frac{2f_y}{b_w E} - \frac{2f_y}{b_f E} = \frac{2f_y}{E} \left(\frac{b_f - b_w}{b_w b_f} \right)$

$$M_y = \frac{1}{2} f_y \left[b_f^2 - \left(2 \frac{f_y}{\phi_y E} \right)^2 \right] t + \frac{f_y}{6} \left(2 \frac{f_y}{\phi_y E} \right)^2 t + \frac{\phi_y E}{12} b_w^3 (h - 2t) \quad (2.12)$$

$$+ \text{Case } \phi_y > \frac{2f_y}{b_w E}, M_y = \frac{1}{4} \cdot h \cdot f_y \cdot b_w^2 - \frac{1}{3} \cdot \frac{h \cdot f_y^3}{\theta^2 \cdot E^2} + \frac{1}{2} \cdot t \cdot f_y \cdot (b_f^2 - b_w^2) \quad (2.13)$$

$$- \text{Maximum moment value: } M_{y,\max} = [2b_f^2 t + b_w^2 (h - 2t)] f_y / 4 \quad (2.14)$$

2.2. Building moment - curvature relationship of composite section beam by the analytical method

Use nonlinear material model of concrete. To determine the moment M^+ , M^- of the composite section beam, it is necessary to determine the moment of each component of M_c concrete slab, M_a floor reinforcement and M_s steel beam, then recombine.

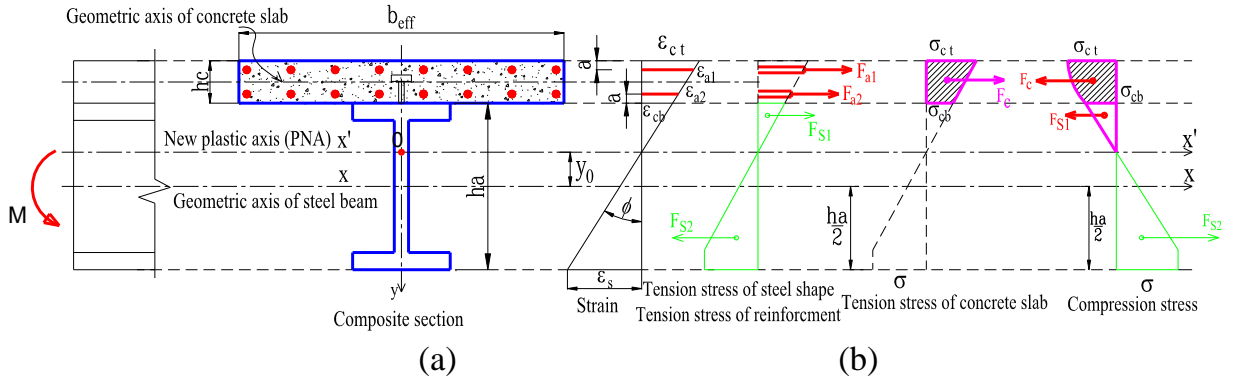


Figure 2.2. Stress and deformation diagram of composite section beam in the main axis

The position of the new plastic neutralizing axis (PNA) y_0 : determined from the equilibrium condition shown in Figure 2.2 with the equilibrium equation:

$$F_c + F_a + F_{s1} + F_{s2} - F_{rc} = 0 \quad (2.15)$$

$$M = M_c + M_a + M_s + M_{rc} \quad (2.16)$$

2.2.1. Considering concrete slab component

When the concrete slab is working, the deformation of points on the bottom of the slab ε_i (ε_{cb}) and the top of the slab ε_j (ε_{ct}) can be achieved in stress positions (points A, B) on chart $\sigma_c - \varepsilon_c$ of concrete material as shown in Figure 2.3. From the deformation of those positions, we can determine the integral area on the chart $\sigma_c - \varepsilon_c$ of the material and determine the components F_c , M_c of concrete slabs.

- Case of tension concrete

$$F_c = b_f \cdot \int_{y_1}^{y_2} 0,5 E_c \phi y dy; F_c = b_f \cdot \int_{y_1}^{y_2} [f_{ct} - 0,8 E_c (\phi y - \varepsilon_{c1})] dy; F_c = b_f \cdot \int_{y_1}^{y_2} [0,5 f_{ct} - 0,075 E_c (\phi y - \varepsilon_{c2})] dy \quad (2.17)$$

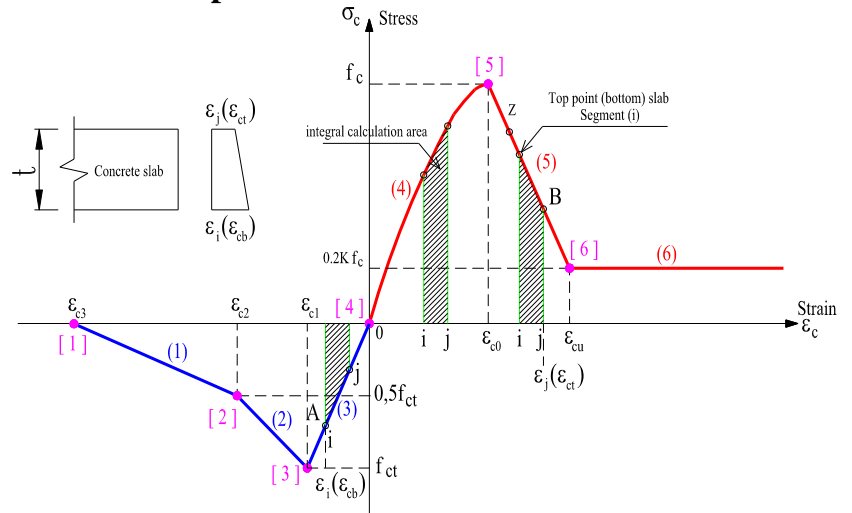


Figure 2.3. The integral area on the chart $\sigma_c - \varepsilon_c$ of the concrete material

$$M_c = b_f \int_{y_1}^{y_2} 0,5E_c \phi y y dy ; M_c = b_f \int_{y_1}^{y_2} [f_{ct} - 0,8E_c(\phi y - \varepsilon_{c1})] y dy ; \quad (2.18)$$

$$M_c = b_f \int_{y_1}^{y_2} [0,5f_{ct} - 0,075E_c(\phi y - \varepsilon_{c2})] y dy \quad (2.19)$$

- Case of compression concrete

$$F_c = b_f \int_{y_1}^{y_2} f_c \left[2 \frac{\phi y}{\varepsilon_0} - \left(\frac{\phi y}{\varepsilon_0} \right)^2 \right] dy ; F_c = b_f \int_{y_1}^{y_2} f_c [1 - Z(\phi y - \varepsilon_0)] dy ; F_c = b_f \int_{y_1}^{y_2} 0,2 f_c dy \quad (2.20)$$

$$M_c = b_f \int_{y_1}^{y_2} f_c \left[2 \frac{\phi y}{\varepsilon_0} - \left(\frac{\phi y}{\varepsilon_0} \right)^2 \right] y dy ; M_c = b_f \int_{y_1}^{y_2} f_c [1 - Z(\phi y - \varepsilon_0)] y dy ; M_c = b_f \int_{y_1}^{y_2} 0,2 f_c y dy \quad (2.21)$$

2.2.2. Considering steel beam component

- Case of compression steel

$$F_{si} = b_i \int_{y_1}^{y_2} E_s \phi y dy ; F_{si} = b_i \int_{y_1}^{y_2} f_s dy ; M_{si} = b_i \int_{y_1}^{y_2} E_s \phi y y dy ; M_{si} = b_i \int_{y_1}^{y_2} f_s y dy \quad (2.22)$$

- Case of tension steel

$$F_{si} = b_i \int_{y_1}^{y_2} E_s \phi y dy ; F_{si} = b_i \int_{y_1}^{y_2} f_s dy ; M_{si} = b_i \int_{y_1}^{y_2} E_s \phi y y dy ; M_{si} = b_i \int_{y_1}^{y_2} f_s y dy \quad (2.23)$$

2.2.3. Considering reinforcement slab component

- Case of compression reinforcement

$$F_a = a_s E_s \phi y ; M_a = a_s E_s \phi y^2 \text{ khi } \varepsilon < \varepsilon_{s1} ; F_a = a_s f_y ; M_a = a_s f_y y \text{ when } \varepsilon \geq \varepsilon_{s1} \quad (2.24)$$

- Case of tension reinforcement

$$F_a = a_s E_s \phi y ; M_a = a_s E_s \phi y^2 \text{ khi } \varepsilon < \varepsilon_{s3} ; F_a = a_s f_y ; M_a = a_s f_y y \text{ when } \varepsilon \geq \varepsilon_{s3} \quad (2.25)$$

2.3. Diagram of SPH program building M-φ of the composite beam by the analytical method.

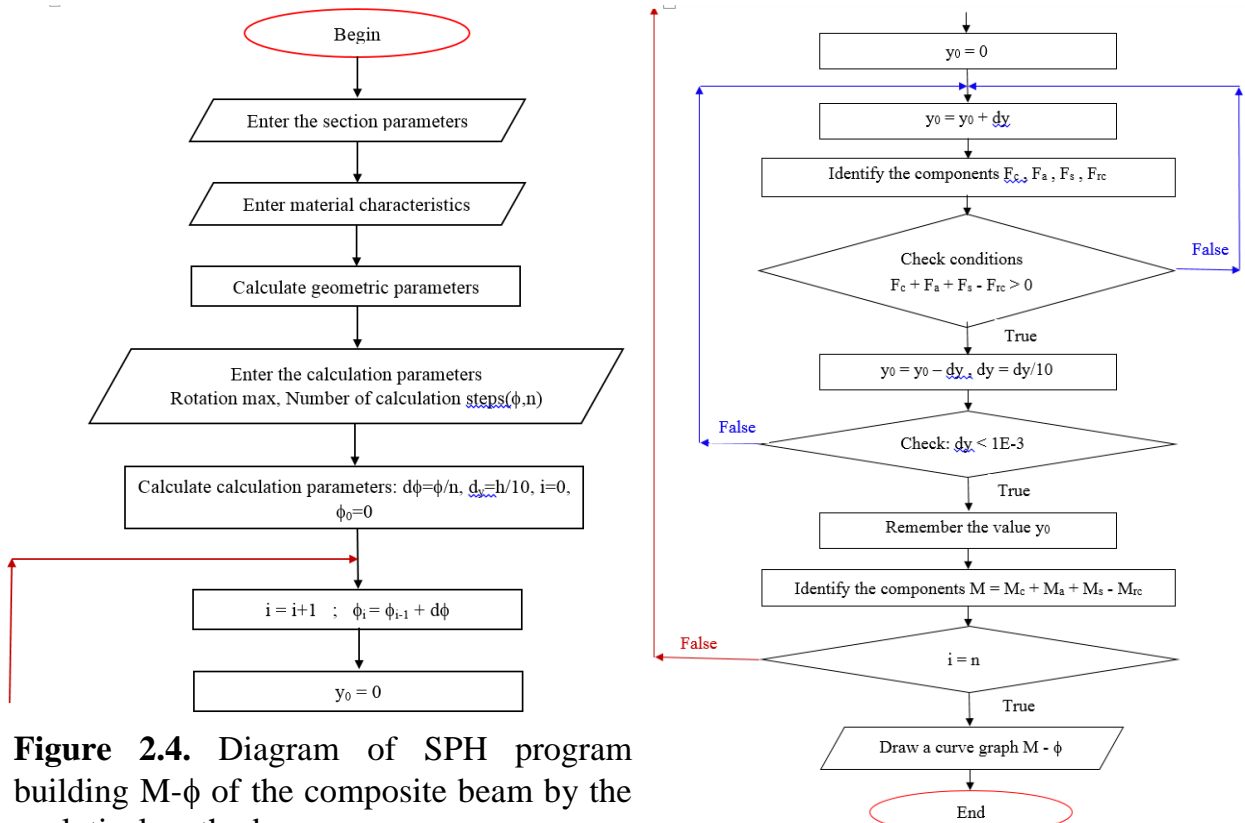


Figure 2.4. Diagram of SPH program building M-φ of the composite beam by the analytical method.

2.4. Building the equation of elastic limit surface of I-section under axial force combined with biaxial bending moments by analytical method

Building the equation of elastic limit surface, intermediate plastic surface, fully plastic surface (failure surface) of the doubly symmetrical wide flange I-section under axial force combined with biaxial bending moments

2.4.1. Building the equation of elastic limit surface (P-M_z) of I-section supported compression and bending in main plane

- Maximum axial force: $P_{\max} = f_y b_w (h-2t) + 2f_y b_f t = A f_y$ (2.26)

- Maximum moment without axial force: $M_{z,\max} = 2 \left[\frac{f_y b_w}{2} \left(\frac{h}{2} - t \right)^2 + \frac{f_y b_f t}{2} (h-t) \right]$ (2.27)

- Maximum moment with axial force:

Case 1: $P \leq b_w (h-2t) f_y$ then $M_z = f_y b_f t (h-t) + \frac{f_y b_w}{4} (h-2t)^2 - \frac{1}{4f_y b_w} P^2$ (2.28)

Case 2: $b_w (h-2t) f_y < P \leq f_y b_w (h-2t) + 2f_y b_f t$

$$M_z = 2f_y \left[\frac{1}{2} b_f \left(t - \frac{1}{2} \frac{P - f_y b_w (h-2t)}{f_y b_f} \right) \left(\frac{1}{2} \frac{P - f_y b_w (h-2t)}{f_y b_f} + h-t \right) \right] \quad (2.29)$$

2.4.2. Building the equation of elastic limit surface (P-M_y) of I-section supported compression and bending in auxiliary plane

- Maximum moment without axial force: $M_{y,\max} = \frac{1}{4} [A_f b_f f_y + A_w b_w f_y]$ (2.30)

- Maximum moment with axial force:

Case 1: $P \leq b_w h f_y$ then $M_y = 2f_y \left[\frac{t}{4} \left(b_f - \frac{P}{f_y h} \right) \left(b_f + \frac{P}{f_y h} \right) + \frac{(h-2t)}{8} \left(b_w - \frac{P}{f_y h} \right) \left(b_w + \frac{P}{f_y h} \right) \right]$

Case 2: $b_w h f_y < P \leq f_y b_w (h-2t) + 2f_y b_f t$ (2.31)

$$M_y = 2f_y \left[t \left(\frac{b_f}{2} - \frac{P - f_y b_w (h-2t)}{4f_y t} \right) \left(\frac{b_f}{2} + \frac{P - f_y b_w (h-2t)}{4f_y t} \right) \right] \quad (2.32)$$

2.4.3. Building the equation of fully plastic surface (failure surface) (P-M_z-M_y-α) of I-section supported axial force combined with biaxial bending moments

Investigation of I-section subjected to P-M_z-M_y as Figure 2.5. To determine the relationship P-M_z-M_y-α, separate the stresses caused by P, M_z and M_y. The new plastic axis NA will divide the section into compression and tension areas. Based on the angle α and the force P to determine the distance y₀ (d), from that the cases of new plastic axis (NA) are determined as shown in Table 2.1. From the position of new plastic axis NA, M_z, M_y value is determined.

The coordinates of points in the new coordinate system with respect to the coordinates of points in the old coordinate system are:

$$\bar{z} = z \cos \alpha + y \sin \alpha, \quad \bar{y} = -z \sin \alpha + y \cos \alpha.$$

Algorithm for calculating the moment M_y and M_z when knowing the axial force P is as follows: determining the axial force values P_i corresponding to the points there $\bar{y}_i > 0$; arranged in ascending axial force $P_i < P_{i+1}$; find the position of P in the list: $P_i \leq P < P_{i+1}$; interpolate to find the distance d corresponding to P; determining M_y and M_z from d values → determining P-M_z-M_y-α relation.

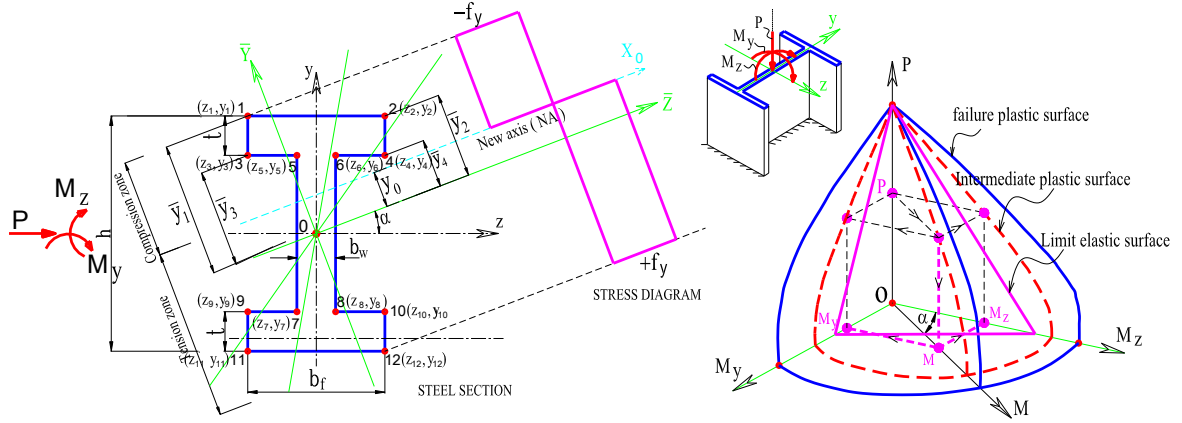


Figure 2.5. Steel section column, stress diagram and plastic surface of I steel section column

Table 2.1. The general cases of the neutral axis correspond to the angle α

Neutral axis cases can occur with the I-shaped section				
CASE 1	CASE 2	CASE 3	CASE 4	
CASE 5	CASE 6	Web TH1	Web TH2	Web TH3

2.4.4. Elastic limit surface (P - M_{ze0} - M_{ye0} - α) of I-section supported axial force combined with biaxial bending moments

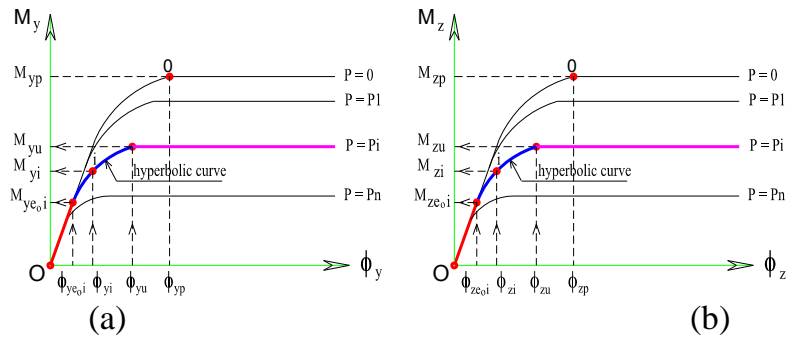
$$p + m_{ye0} + m_{ze0} = 1; M_{ye} = W_y f_y; M_{ze} = W_z f_y \quad (2.33)$$

$$M_{ye0} = m_{ye0} M_{ye} = f_y \frac{1-p}{\frac{h}{b_f} + \tan \alpha} \tan \alpha W_y; M_{ze0} = m_{ze0} M_{ze} = f_y \frac{1-p}{1 + \frac{b_f}{h} \tan \alpha} W_z \quad (2.34)$$

2.4.5. The relationship equation M_y - P - ϕ_y ; M_z - P - ϕ_z curved segment transition from elastic to fully plastic as shown in Figure 2.6

$$M_y = M_{ye0} + \frac{\phi_y - \phi_{ye0}}{\frac{1}{EI_y} + \frac{\phi_y - \phi_{ye0}}{M_{yu} - M_{ye0}}}; M_z = M_{ze0} + \frac{\phi_z - \phi_{ze0}}{\frac{1}{EI_z} + \frac{\phi_z - \phi_{ze0}}{M_{zu} - M_{ze0}}} \quad (2.35)$$

Figure 2.6. (a) - relationship curve $M_y - P - \phi_y$;
(b) - relationship curve $M_z - P - \phi_z$



For each value of p , there is the p - m_z - m_y relation of the fully plastic surface which is the horizontal section of the fully plastic cross section of W14x426 steel column shown in Figure 2.8 and the elastic limit surface as shown in Figure 2.7. If the force point is inside the p - m_z - m_y elastic limit line, the section is still elastic, if the point is located between the elastic limit line and the fully plastic curve, the section will yield partially, if the point the force outside the p - m_z - m_y fully plastic curve is completely broken. This has practical implications when testing the bearing capacity of steel cross section (Figure 2.10).

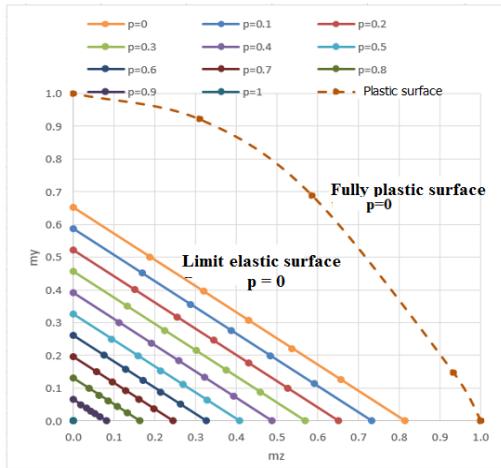


Figure 2.7. section of elastic limit surface $m_y - m_z - p - \alpha - (\phi=0)$ of W14x426 steel column section by analytical method

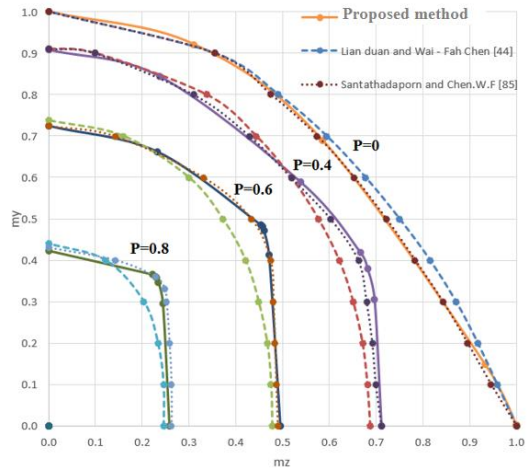


Figure 2.8. Comparison of section of fully plastic surface $m_y - m_z - p - \alpha - \phi$ of W14x426 steel column section by proposed method and other studies

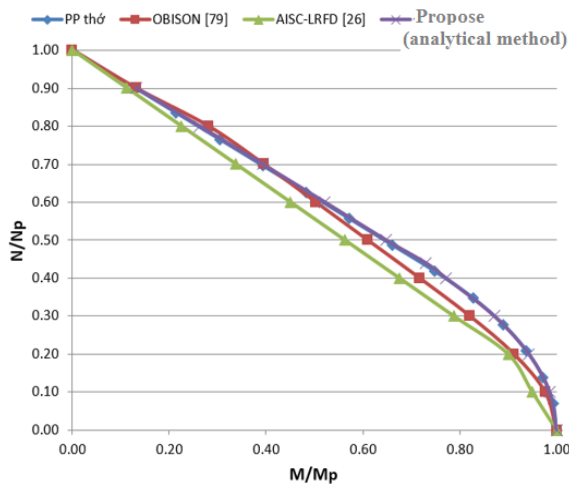


Figure 2.9. Comparison of fully plastic surface $P - M_z$ of steel column cross section

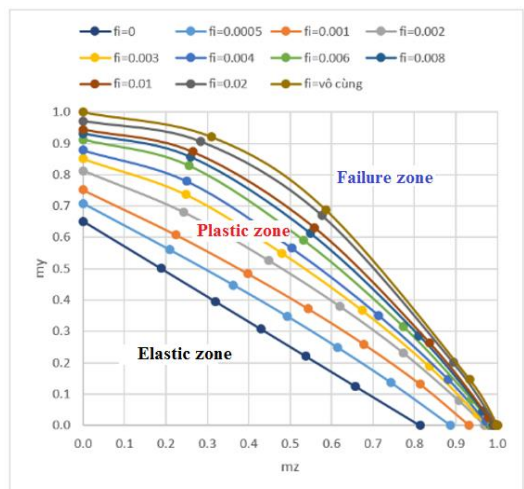


Figure 2.10. Elastic limite, intermediate plastic, fully plastic surface of steel column

W14x426 by analytical method and other studies

cross section W14x426 by analytical method ($p=0$)

From Figures 2.8 and 2.9, it is shown that the plastic surfaces of different studies and the proposed plastic surfaces are approximately identical, so the proposed plastic surface was constructed by analytical method with high reliability.

CHAPTER 3: A FINITE ELEMENTS METHOD OF ANALYSIS STRUCTURE WITH STEEL COLUMN AND COMPOSITE STEEL – CONCRETE BEAM CONSIDERS THE DISTRIBUTED PLASTICITY OF THE ELEMENTS

3.1. Assumptions when performing analytical problems

All the bar elements of the structural system when unloaded are straight and have a constant cross-sectional area. When the bar elements are flexible, the cross section is still flat and orthogonal to the x-axis (the local coordinate system of the element); plastic deformation that appears and develops in elements of a structure is distributed plastic deformation, so plastic deformation can exist in all sections during load bearing process; deformation and displacement of the structural system are small, ignoring nonlinear geometry; The link between concrete floor and steel girder is fully bonded; Ignore displacements due to shear distortion; consider only flexible working materials, bypassing the consolidation stage.

3.2. Building plastic multi point beam – column elements

The author of the thesis proposes a plastic multi-point beam-column element as shown in Figures 3.1 and 3.2. Model of girder element is an element with only two nodes with two ends of the element, assuming there are n continuous plastic deformation points inside the element (flexible plastic points), each segment of $x_i - x_{i+1}$ consists of two consecutive plastic deformation points and this segment has the stiffness $EI_i(x)$ varies with the function of degree 3 (see appendix 2), the stiffness $EI_i(x_i)$ is determined through the moment-curvature relationship curve (M- ϕ -P). With this proposed element, it is not necessary to divide the element into many sub-elements as some studies have done. Using plastic multi-point bar elements has the advantage of giving accurate results compared to the actual working of the structure, significantly reducing the size of the structural analysis problem, increasing the calculation speed quickly, giving know the plastic flow rate of the section, the order of formation of plastic joints and the flexible plastic behavior of the entire structure, from which it is possible to predict and evaluate the reserve or safety of the structure. The location of flexible joints in any bar depends on the plastic flow of the section during structural analysis. Model of girder, flexible multi-point columns are shown in Figure 3.1, 3.2.

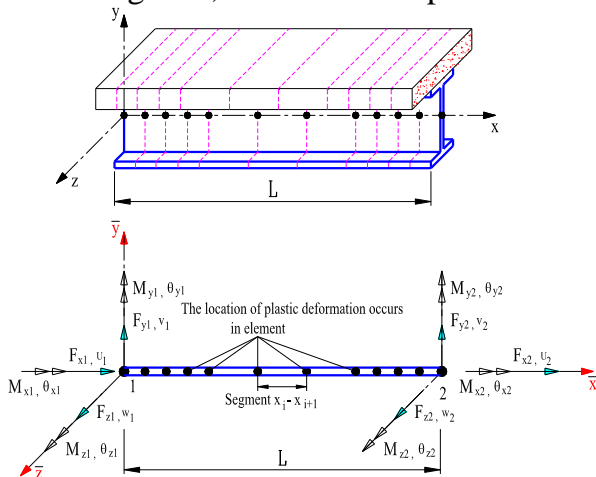


Figure 3.1. Phần tử dầm liên hợp đa điểm dẻo

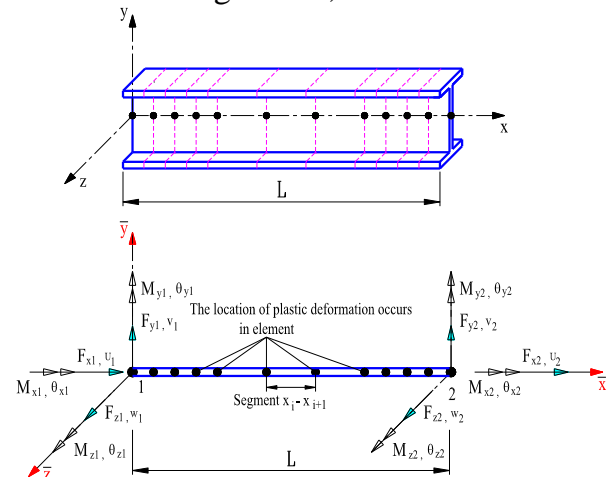


Figure 3.2. Phần tử cột thép đa điểm dẻo

3.3. Building stiffness matrix of composite beam, plastic multi-point plane column when mentioning the the distributed plasticity along element length

Assuming there are n continuous plastic deformation points inside the element, the number and distribution of plastic points are set by the user on each element and according to the law of uniform distribution over the element length as shown in Figure 3.1. Each segment $x_i - x_{i+1}$ consists of two consecutive plastic deformation points and this segment has the stiffness $EI_z(x)$ varies with the function of order 3

$$EI_z(x) = (ax + b)^3, \text{ where: } a = \left(\sqrt[3]{EI'_{i+1}} - \sqrt[3]{EI'_i} \right) / L; b = \sqrt[3]{EI'_i}. \quad (3.1)$$

Considering any element with 2 nodes 1 (the first node) and 2 (the last node) with internal forces and displacements as shown in Figure 3.3, establish the knot force relationship of the element. Determine the offset energy of deformation:

$$U^* = \sum_{i=1}^{n-1} \frac{1}{2} \int_{x_i}^{x_{i+1}} \frac{(M_x)^2}{EI_z(x)} dx = \sum_{i=1}^{n-1} \frac{1}{2} \int_{x_i}^{x_{i+1}} \frac{(V_1 x - M_1)^2}{EI_z(x)} dx \quad (3.2)$$

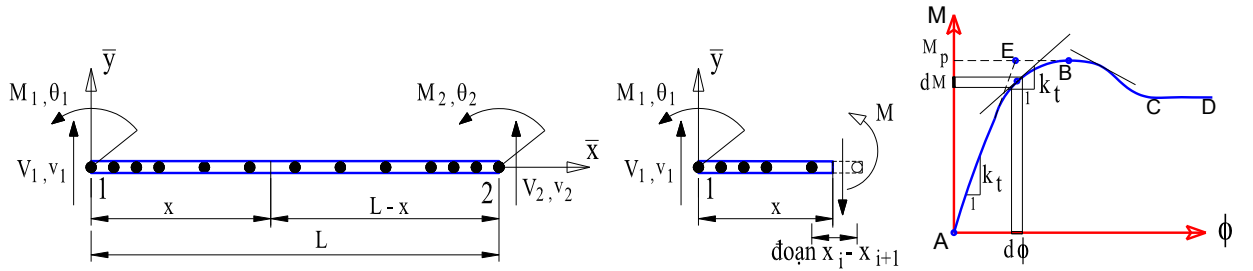


Figure 3.3. The force of the bar and the tangent stiffness at the position have plastic deformation

Apply the Engesser theorem and solve the equation: $dU^* / dV_1 = v_1$; $dU^* / dM_1 = \theta_1$; identify values M_1, V_1, M_2, V_2 of each node. From the internal force results M_1, V_1, M_2, V_2 at the first and end nodes of the element and based on the equilibrium equation: $NL = [k_e] \cdot \{u\}$, arrange the stiffness components into the stiffness matrix of composite beam elements, flexible multi-point plane column. The result is the stiffness matrix as shown in formula 3.3. Stiffness EI'_i (k_t) - tangent stiffness at the position of plastic deformation, with beams determined through the $M-\phi$ relationship curve as shown in Figure 3.3, with columns determined through P-M- ϕ in Figure 2.6.

$$[k_p^d]([k_p^{2d}]) = \begin{bmatrix} k_{11} & 0 & 0 & k_{14} & 0 & 0 \\ 0 & k_{22} & k_{23} & 0 & k_{25} & k_{26} \\ 0 & k_{32} & k_{33} & 0 & k_{35} & k_{36} \\ k_{41} & 0 & 0 & k_{44} & 0 & 0 \\ 0 & k_{52} & k_{53} & 0 & k_{55} & k_{56} \\ 0 & k_{62} & k_{63} & 0 & k_{65} & k_{66} \end{bmatrix} \quad (3.3)$$

Where: The components in the matrix (3.19b) are determined as follows: $k_{11} = k_{44} = 1 / \sum_{i=1}^{n-1} \int_{x_i}^{x_{i+1}} \frac{1}{EA(x)} dx$

$$A(x) = A_i + (A_{i+1} - A_i) \frac{x}{L}$$

$$k_{14} = k_{41} = -1 / \sum_{i=1}^{n-1} \int_{x_i}^{x_{i+1}} \frac{1}{EA(x)} dx$$

$$\text{Put } B_z = \sum_{i=1}^{n-1} \int_{x_i}^{x_{i+1}} \frac{x^2}{EI_z(x)} dx \cdot \sum_{i=1}^{n-1} \int_{x_i}^{x_{i+1}} \frac{1}{EI_z(x)} dx - \sum_{i=1}^{n-1} \int_{x_i}^{x_{i+1}} \frac{x}{EI_z(x)} dx \cdot \sum_{i=1}^{n-1} \int_{x_i}^{x_{i+1}} \frac{x}{EI_z(x)} dx$$

$$\text{Put } C_z = \sum_{i=1}^{n-1} \int_{x_i}^{x_{i+1}} \frac{L^2 - 2Lx + x^2}{EI_z(x)} dx \cdot \sum_{i=1}^{n-1} \int_{x_i}^{x_{i+1}} \frac{1}{EI_z(x)} dx - \sum_{i=1}^{n-1} \int_{x_i}^{x_{i+1}} \frac{L-x}{EI_z(x)} dx \cdot \sum_{i=1}^{n-1} \int_{x_i}^{x_{i+1}} \frac{L-x}{EI_z(x)} dx$$

$$\begin{aligned}
k_{22} &= \frac{\sum_{i=1}^{n-1} \int_{x_i}^{x_{i+1}} \frac{1}{EI_z(x)} dx}{B_z}; k_{23} = k_{32} = \frac{\sum_{i=1}^{n-1} \int_{x_i}^{x_{i+1}} \frac{x}{EI_z(x)} dx}{B_z}; k_{25} = k_{52} = -\frac{\sum_{i=1}^{n-1} \int_{x_i}^{x_{i+1}} \frac{1}{EI_z(x)} dx}{C_z}; k_{26} = k_{62} = -\frac{\sum_{i=1}^{n-1} \int_{x_i}^{x_{i+1}} \frac{L-x}{EI_z(x)} dx}{C_z} \\
k_{33} &= \frac{\sum_{i=1}^{n-1} \int_{x_i}^{x_{i+1}} \frac{x^2}{EI_z(x)} dx}{B_z}; k_{35} = k_{53} = \frac{-\sum_{i=1}^{n-1} \int_{x_i}^{x_{i+1}} \frac{x}{EI_z(x)} dx}{C_z}; k_{36} = k_{63} = \frac{\sum_{i=1}^{n-1} \int_{x_i}^{x_{i+1}} \frac{Lx-x^2}{EI_z(x)} dx}{C_z}; k_{55} = \frac{\sum_{i=1}^{n-1} \int_{x_i}^{x_{i+1}} \frac{1}{EI_z(x)} dx}{C_z}; \\
k_{56} = k_{65} &= \frac{-\sum_{i=1}^{n-1} \int_{x_i}^{x_{i+1}} \frac{L-x}{EI_z(x)} dx}{C_z}; k_{66} = \frac{\sum_{i=1}^{n-1} \int_{x_i}^{x_{i+1}} \frac{L^2-2Lx+x^2}{EI_z(x)} dx}{C_z}; k_{ii} = EI_i^t = dM_i / d\phi_i; k_{t(i+1)} = EI_{i+1}^t = dM_{i+1} / d\phi_{i+1}
\end{aligned}$$

3.4. Building stiffness matrix of 3D column elements when mentioning the the distributed plasticity along element length

Building similar to the plastic multi-point column having a stiffness matrix of 12x12 of the 3D plastic multi-point column element when mentioning the the distributed plasticity along element length as formula 3.4.

$$\left[k_p^{3d} \right] = \begin{bmatrix} k_{11} & 0 & 0 & 0 & 0 & 0 & k_{17} & 0 & 0 & 0 & 0 & 0 \\ 0 & k_{22} & 0 & 0 & 0 & k_{26} & 0 & k_{28} & 0 & 0 & 0 & k_{212} \\ 0 & 0 & k_{33} & 0 & k_{35} & 0 & 0 & 0 & k_{39} & 0 & k_{311} & 0 \\ 0 & 0 & 0 & k_{44} & 0 & 0 & 0 & 0 & 0 & k_{410} & 0 & 0 \\ 0 & 0 & k_{53} & 0 & k_{55} & 0 & 0 & 0 & k_{59} & 0 & k_{511} & 0 \\ 0 & k_{62} & 0 & 0 & 0 & k_{66} & 0 & k_{68} & 0 & 0 & 0 & k_{612} \\ k_{71} & 0 & 0 & 0 & 0 & 0 & k_{77} & 0 & 0 & 0 & 0 & 0 \\ 0 & k_{82} & 0 & 0 & 0 & k_{86} & 0 & k_{88} & 0 & 0 & 0 & k_{812} \\ 0 & 0 & k_{93} & 0 & k_{95} & 0 & 0 & 0 & k_{99} & 0 & k_{911} & 0 \\ 0 & 0 & 0 & k_{104} & 0 & 0 & 0 & 0 & 0 & k_{1010} & 0 & 0 \\ 0 & 0 & k_{113} & 0 & k_{115} & 0 & 0 & 0 & k_{119} & 0 & k_{1111} & 0 \\ 0 & k_{122} & 0 & 0 & 0 & k_{126} & 0 & k_{128} & 0 & 0 & 0 & k_{1212} \end{bmatrix} \quad \begin{aligned} k_{44} &= k_{1010} = \frac{GI_T}{L} \\ k_{104} &= k_{410} = -\frac{GI_T}{L} \\ k_{11} &= k_{77} = 1 / \sum_{i=1}^{n-1} \int_{x_i}^{x_{i+1}} \frac{1}{EA(x)} dx \\ k_{17} &= k_{71} = -1 / \sum_{i=1}^{n-1} \int_{x_i}^{x_{i+1}} \frac{1}{EA(x)} dx \\ k_{22} &= \frac{\sum_{i=1}^{n-1} \int_{x_i}^{x_{i+1}} \frac{1}{EI_z(x)} dx}{B_z} \end{aligned} \quad (3.4)$$

$$\text{Put } B_y = \sum_{i=1}^{n-1} \int_{x_i}^{x_{i+1}} \frac{x^2}{EI_y(x)} dx; \sum_{i=1}^{n-1} \int_{x_i}^{x_{i+1}} \frac{1}{EI_y(x)} dx - \sum_{i=1}^{n-1} \int_{x_i}^{x_{i+1}} \frac{x}{EI_y(x)} dx; \sum_{i=1}^{n-1} \int_{x_i}^{x_{i+1}} \frac{x}{EI_y(x)} dx;$$

$$\text{Put } C_y = \sum_{i=1}^{n-1} \int_{x_i}^{x_{i+1}} \frac{L^2-2Lx+x^2}{EI_y(x)} dx; \sum_{i=1}^{n-1} \int_{x_i}^{x_{i+1}} \frac{1}{EI_y(x)} dx - \sum_{i=1}^{n-1} \int_{x_i}^{x_{i+1}} \frac{L-x}{EI_y(x)} dx; \sum_{i=1}^{n-1} \int_{x_i}^{x_{i+1}} \frac{L-x}{EI_y(x)} dx;$$

$$k_{26} = k_{62} = \frac{\sum_{i=1}^{n-1} \int_{x_i}^{x_{i+1}} \frac{x}{EI_z(x)} dx}{B_z}; k_{28} = k_{82} = -\frac{\sum_{i=1}^{n-1} \int_{x_i}^{x_{i+1}} \frac{1}{EI_z(x)} dx}{C_z}; k_{212} = k_{122} = -\frac{-\sum_{i=1}^{n-1} \int_{x_i}^{x_{i+1}} \frac{L-x}{EI_z(x)} dx}{C_z}; k_{66} = \frac{\sum_{i=1}^{n-1} \int_{x_i}^{x_{i+1}} \frac{x^2}{EI_z(x)} dx}{B_z}$$

$$k_{68} = k_{86} = \frac{-\sum_{i=1}^{n-1} \int_{x_i}^{x_{i+1}} \frac{x}{EI_z(x)} dx}{C_z}; k_{612} = k_{126} = \frac{\sum_{i=1}^{n-1} \int_{x_i}^{x_{i+1}} \frac{Lx-x^2}{EI_z(x)} dx}{C_z}; k_{88} = \frac{\sum_{i=1}^{n-1} \int_{x_i}^{x_{i+1}} \frac{1}{EI_z(x)} dx}{C_z}; k_{812} = k_{128} = \frac{-\sum_{i=1}^{n-1} \int_{x_i}^{x_{i+1}} \frac{L-x}{EI_z(x)} dx}{C_z}$$

$$k_{1212} = \frac{\sum_{i=1}^{n-1} \int_{x_i}^{x_{i+1}} \frac{L^2-2Lx+x^2}{EI_z(x)} dx}{C_z}; k_{33} = \frac{\sum_{i=1}^{n-1} \int_{x_i}^{x_{i+1}} \frac{1}{EI_y(x)} dx}{B_y}; k_{35} = k_{53} = -\frac{\sum_{i=1}^{n-1} \int_{x_i}^{x_{i+1}} \frac{x}{EI_y(x)} dx}{B_y}; k_{39} = k_{93} = -\frac{\sum_{i=1}^{n-1} \int_{x_i}^{x_{i+1}} \frac{1}{EI_y(x)} dx}{C_y}$$

$$k_{311} = k_{113} = \frac{-\sum_{i=1}^{n-1} \int_{x_i}^{x_{i+1}} \frac{L-x}{EI_y(x)} dx}{C_y}; k_{55} = \frac{\sum_{i=1}^{n-1} \int_{x_i}^{x_{i+1}} \frac{x^2}{EI_y(x)} dx}{B_y}; k_{59} = k_{95} = -\frac{-\sum_{i=1}^{n-1} \int_{x_i}^{x_{i+1}} \frac{x}{EI_y(x)} dx}{C_y}; k_{99} = \frac{\sum_{i=1}^{n-1} \int_{x_i}^{x_{i+1}} \frac{1}{EI_y(x)} dx}{C_y}$$

$$k_{511} = k_{115} = \frac{\sum_{i=1}^{n-1} \int_{x_i}^{x_{i+1}} \frac{Lx - x^2}{EI_y(x)} dx}{C_y}; k_{911} = k_{119} = -\frac{-\sum_{i=1}^{n-1} \int_{x_i}^{x_{i+1}} \frac{L-x}{EI_y(x)} dx}{C_y}; k_{1111} = \frac{\sum_{i=1}^{n-1} \int_{x_i}^{x_{i+1}} \frac{L^2 - 2Lx + x^2}{EI_y(x)} dx}{C_y};$$

Tangent stiffness EI_{it} (k_{it}) is determined as follows:

$$(EI_y)_t = \frac{\partial M_y}{\partial \phi_y} = EI_y \left(\frac{M_{yu} - M_y}{M_{yu} - M_{ye0}} \right)^2; (EI_z)_t = \frac{\partial M_z}{\partial \phi_z} = EI_z \left(\frac{M_{zu} - M_z}{M_{zu} - M_{ze0}} \right)^2 \quad (3.5)$$

3.5. The converted load vector of a plastic multi-point bar element has a continuous plastic deformation point along the element length

3.1.1.. The load is distributed on plastic multi-point bar elements

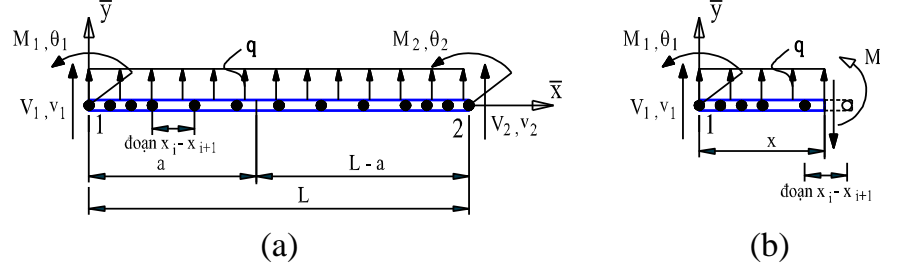


Figure 3.4.(a)The distributed load on elements (b) the knot force relationship of the beam bar

From Figure 3.4b there is a relationship of knot force of beams as follows:

$$M(x) = V_1 x - M_1 + 0.5qx^2$$

$$\text{Determine the compensatory energy of the deformation: } U^* = \sum_{i=1}^{n-1} \frac{1}{2} \int_{x_i}^{x_{i+1}} \frac{(M_x)^2}{EI_z(x)} dx \quad (3.6)$$

Apply the Engesser theorem and solve equations: $\frac{dU^*}{dV_1} = v_1 = 0$; $\frac{dU^*}{dM_1} = \theta_1 = 0$ identify values

M_1, V_1, M_2, V_2 of each node.

$$M_1 = \frac{1}{2} q \frac{\sum_{i=1}^{n-1} \int_{x_i}^{x_{i+1}} \frac{x^3}{EI_z(x)} dx \sum_{i=1}^{n-1} \int_{x_i}^{x_{i+1}} \frac{x}{EI_z(x)} dx - \sum_{i=1}^{n-1} \int_{x_i}^{x_{i+1}} \frac{x^2}{EI_z(x)} dx \sum_{i=1}^{n-1} \int_{x_i}^{x_{i+1}} \frac{x^2}{EI_z(x)} dx}{\sum_{i=1}^{n-1} \int_{x_i}^{x_{i+1}} \frac{x}{EI_z(x)} dx \sum_{i=1}^{n-1} \int_{x_i}^{x_{i+1}} \frac{x}{EI_z(x)} dx - \sum_{i=1}^{n-1} \int_{x_i}^{x_{i+1}} \frac{1}{EI_z(x)} dx \sum_{i=1}^{n-1} \int_{x_i}^{x_{i+1}} \frac{x^2}{EI_z(x)} dx} \quad (3.7)$$

$$V_1 = \frac{1}{2} q \frac{\sum_{i=1}^{n-1} \int_{x_i}^{x_{i+1}} \frac{x^3}{EI_z(x)} dx \sum_{i=1}^{n-1} \int_{x_i}^{x_{i+1}} \frac{1}{EI_z(x)} dx - \sum_{i=1}^{n-1} \int_{x_i}^{x_{i+1}} \frac{x^2}{EI_z(x)} dx \sum_{i=1}^{n-1} \int_{x_i}^{x_{i+1}} \frac{x}{EI_z(x)} dx}{\sum_{i=1}^{n-1} \int_{x_i}^{x_{i+1}} \frac{x}{EI_z(x)} dx \sum_{i=1}^{n-1} \int_{x_i}^{x_{i+1}} \frac{x}{EI_z(x)} dx - \sum_{i=1}^{n-1} \int_{x_i}^{x_{i+1}} \frac{1}{EI_z(x)} dx \sum_{i=1}^{n-1} \int_{x_i}^{x_{i+1}} \frac{x^2}{EI_z(x)} dx} \quad (3.8)$$

$$V_2 = -V_1 - qL; M_2 = V_1 L + \frac{qL^2}{2} - M_1 \quad (3.9)$$

The nodal load vector of a plastic multi-point bar element under a distributed load in a local coordinate system has elements equal to the counterpart but opposite of the jet, as shown in the following formula (3.10): $\{f\} = \{-V_1 \quad -M_1 \quad -V_2 \quad -M_2\}^T$ (3.10)

3.1.2. Consider the concentrated of P_y load on the element

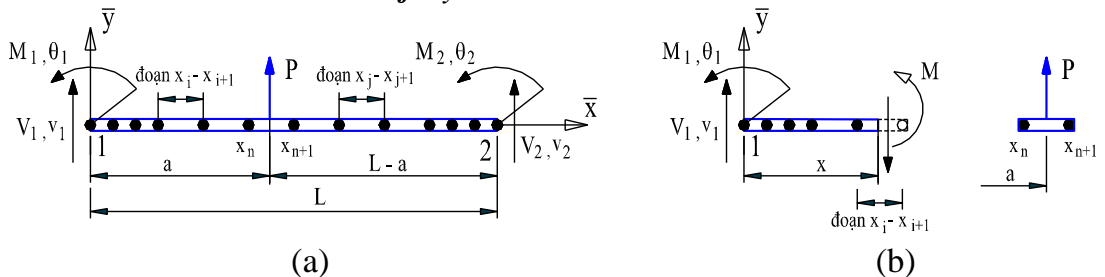


Figure 3.5. (a) - The load is concentrated P_y on elements (b) - the knot force relationship of the beam bar

Consider the concentrated load perpendicular to the bar axis as shown in Figure 3.5a. From Figure 3.5b, there is a relationship between knot force of beams as follows:

$$M(x) = M_1(x) + M_2(x) + M_3(x) + M_4(x) \quad (3.11)$$

the compensatory energy of the deformation:

$$U^* = \sum_{i=1}^{n-1} \frac{1}{2} \int_{x_i}^{x_{i+1}} \frac{(M_x)^2}{EI_z(x)} dx = U_1^* + U_2^* + U_3^* + U_4^* \quad (3.12)$$

$$U^* = \sum_{i=1}^{n-1} \frac{1}{2} \int_{x_i}^{x_{i+1}} \frac{(V_1x - M_1)^2}{EI_z(x)} dx + \frac{1}{2} \int_{x_n}^a \frac{(V_1x - M_1)^2}{EI_z(x)} dx + \frac{1}{2} \int_a^{x_{n+1}} \frac{(V_1x - M_1 + P(x-a))^2}{EI_z(x)} dx + \sum_{j=1}^m \frac{1}{2} \int_{x_j}^{x_{j+1}} \frac{(V_1x - M_1 + P(x-a))^2}{EI_z(x)} dx$$

Apply the Engesser theorem and solve equations: $\frac{dU^*}{dV_1} = v_1 = 0$; $\frac{dU^*}{dM_1} = \theta_1 = 0$ identify values

M_1, V_1, M_2, V_2 of each node.

$$V_1 = \frac{b_2 \cdot c_1 - b_1 \cdot c_2}{a_1 \cdot b_2 - b_1 \cdot a_2}; M_1 = \frac{a_1 \cdot c_2 - a_2 \cdot c_1}{a_1 \cdot b_2 - b_1 \cdot a_2}; V_2 = -V_1 - P; M_2 = V_1L + P(L-a) - M_1 \quad (3.13)$$

$$a_1 = \sum_{i=1}^{n-1} \int_{x_i}^{x_{i+1}} \frac{x^2}{EI_z(x)} dx + \int_{x_n}^a \frac{x^2}{EI_z(x)} dx + \int_a^{x_{n+1}} \frac{x^2}{EI_z(x)} dx + \sum_{j=n+1}^m \int_{x_j}^{x_{j+1}} \frac{x^2}{EI_z(x)} dx \quad (3.14)$$

$$b_1 = -\sum_{i=1}^{n-1} \int_{x_i}^{x_{i+1}} \frac{x}{EI_z(x)} dx - \int_{x_n}^a \frac{x}{EI_z(x)} dx - \int_a^{x_{n+1}} \frac{x}{EI_z(x)} dx - \sum_{j=n+1}^m \int_{x_j}^{x_{j+1}} \frac{x}{EI_z(x)} dx \quad (3.15)$$

$$c_1 = -P \int_a^{x_{n+1}} \frac{(x-a)x}{EI_z(x)} dx - P \sum_{j=n+1}^m \int_{x_j}^{x_{j+1}} \frac{(x-a)x}{EI_z(x)} dx \quad (3.16)$$

$$a_2 = -\sum_{i=1}^{n-1} \int_{x_i}^{x_{i+1}} \frac{x}{EI_z(x)} dx - \int_{x_n}^a \frac{x}{EI_z(x)} dx - \int_a^{x_{n+1}} \frac{x}{EI_z(x)} dx - \sum_{j=n+1}^m \int_{x_j}^{x_{j+1}} \frac{x}{EI_z(x)} dx \quad (3.17)$$

$$b_2 = \sum_{i=1}^{n-1} \int_{x_i}^{x_{i+1}} \frac{1}{EI_z(x)} dx + \int_{x_n}^a \frac{1}{EI_z(x)} dx + \int_a^{x_{n+1}} \frac{1}{EI_z(x)} dx + \sum_{j=n+1}^m \int_{x_j}^{x_{j+1}} \frac{1}{EI_z(x)} dx \quad (3.18)$$

$$c_2 = P \int_a^{x_{n+1}} \frac{(x-a)}{EI_z(x)} dx + P \sum_{j=n+1}^m \int_{x_j}^{x_{j+1}} \frac{(x-a)}{EI_z(x)} dx \quad (3.19)$$

The nodal load vector of a plastic multi-point bar element under the concentrated load in a local coordinate system has elements equal to the counterpart but opposite of the jet, as shown in the following formula (3.10): $\{f\} = \{-V_1 \quad -M_1 \quad -V_2 \quad -M_2\}^T$ (3.10)

3.6. Equation equilibrium for the whole structure

In the general case of elastic-plastic bar structure, the stiffness matrix and the node load vector depend on the state of the bar element with the elastic and plastic nodal points. Therefore, the stiffness matrix and nodal load vectors of a structure system are determined through a set of stiffness matrices and the nodal load vector of the respective plastic point multi-point element. Thus, it can be affirmed that the equation of elastic-plastic structure is the nonlinear equation written in matrix form: $\{F\} = [K] \cdot \{U\}$ where: (3.21)

$[K]$ - stiffness matrix of a structure in a general coordinate system:

$$[K] = [T]^T \cdot [k_p] \cdot [T] \quad (3.22)$$

$\{U\}$ - vector displacement node of the structure in the global coordinate system:

$$\{U\} = [T]^T \cdot \{u\} \quad (3.23)$$

$\{F\}$ - Vector node load of structure in the general coordinate system: $\{F\} = [T]^T \cdot \{f\}$ (3.24)

CHAPTER 4: BUILDING PLASTIC ANALYSIS PROGRAM AND SURVEYING A NUMBER OF PROBLEMS

4.1. Method to solve balanced equations

4.1.1. Nonlinear algorithm

There are three main iterative methods for nonlinear analysis: Simple Euler load algorithm as shown in Figure 4.2 Chan and Chui, Newton-Raphson method as shown in Figure 4.3 and improved Newton-Raphson method as shown in Figure 4.4, Chan and Chui, Robert et al.

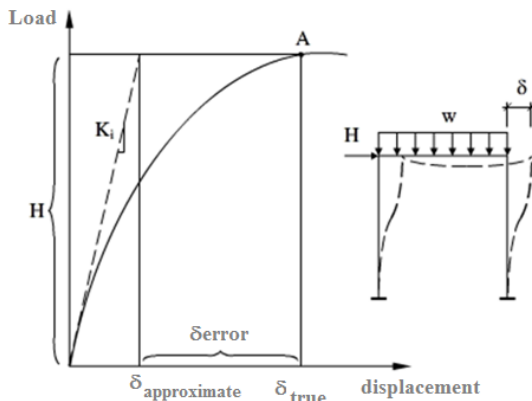


Figure 4.1. Load - displacement behavior of the portal frame is subject to the load

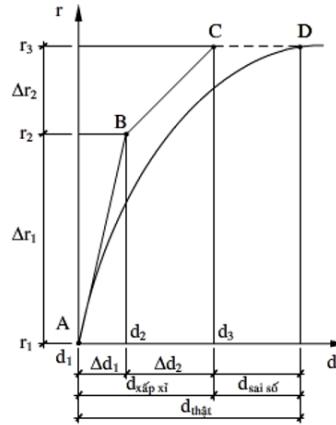


Figure 4.2. Schematic illustration of the simple Euler algorithm

4.1.2. Newton-Raphson and improved Newton-Raphson method

The cumulative error results of the simple incremental technique can be minimized by a combined iteration in each load step during analysis. The iteration minimizes the unbalanced forces between external forces and internal resistance that occur at each load step by the improved Newton-Raphson and Newton-Raphson Method methods as shown in Figure 4.3, 4.4.

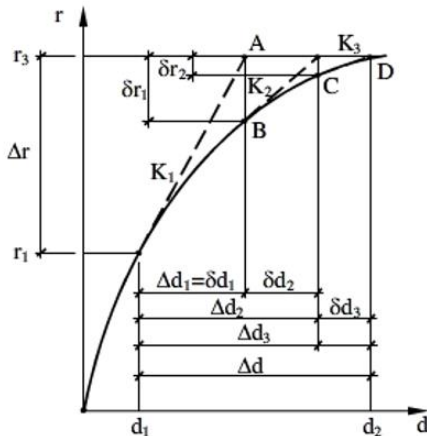


Figure 4.3. Schematic illustration of the Newton-Raphson method

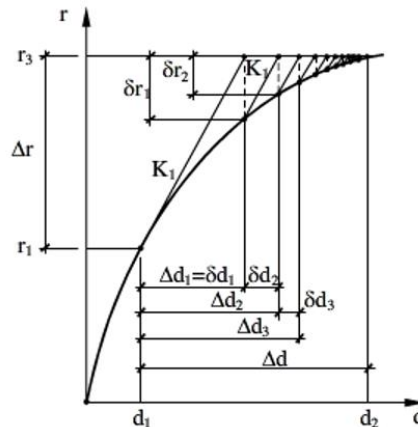


Figure 4.4. Schematic illustration of the improved Newton-Raphson method

4.2. Algorithm diagram of structural plastic analysis and SPH analysis program

Algorithm diagram of SPH program for structural plasticity analysis is shown in Figure 4.5

4.3. Limited load coefficient and plastic flow rate of the section

- Determine the limited load coefficient λ_p of structure:

$$\lambda_p = \text{limited load when system is failed} / \text{Applied load} \quad (4.1)$$

From the coefficient λ_p it is possible to assess the safety level of a structure under load.

- Determine plastic flow rate of the section: % plastic flow = $100\% - EI_t / EI_{max} \times 100\%$ (4.2)

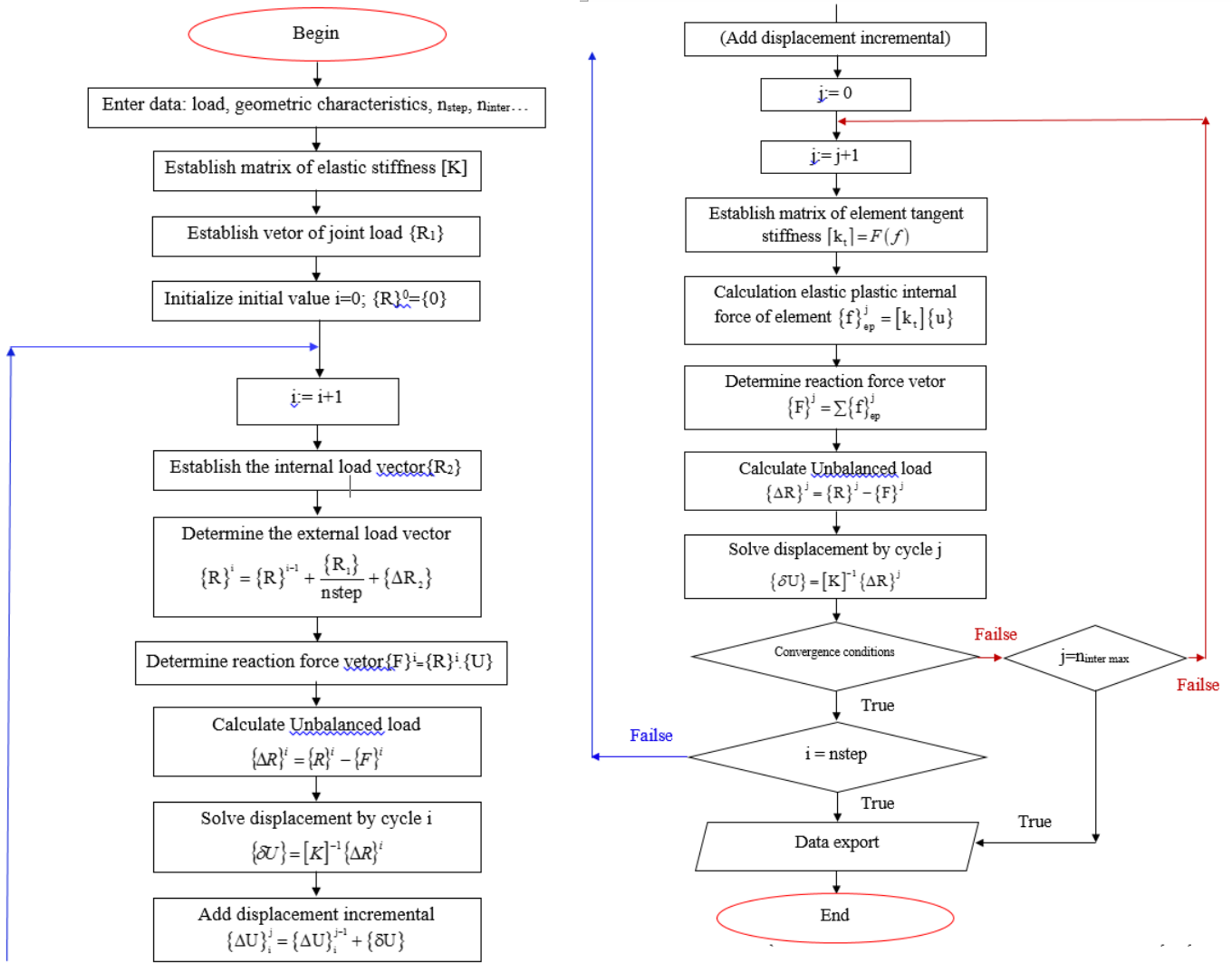
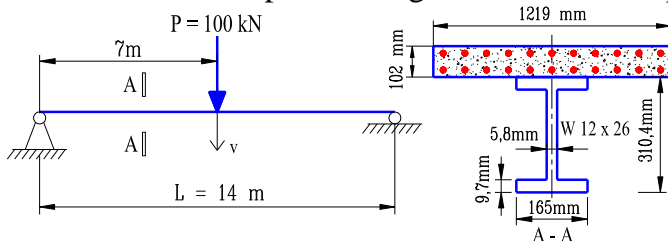


Figure 4.5. Algorithm diagram of structural plastic analysis SPH program

4.4. Survey some plastic analysis problems

4.4.1. Composite steel – concrete simple beam

Investigation of Composite steel - concrete simple beam with girder section including W12x27 steel, 102x1219mm concrete slab as shown in Figure 4.6. The concentrat force is $P = 100 \text{ kN}$ at the center of the beam, the load step is $n_{step} = P/100$. Compressive strength of concrete $f_c' = 16 \text{ MPa}$, $f_{ct} = 1.2 \text{ MPa}$, elastic modulus of concrete $E_b = 32,5 \cdot 10^3 \text{ MPa}$, $\epsilon_0 = 0.002$, $\epsilon_u = 0.004$. Yield stress of beam steel $f_y = 252.4 \text{ MPa}$, tensile strength of reinforcement steel $f_y = 210 \text{ MPa}$, elastic modulus of steel $E_s = 2 \cdot 10^5 \text{ MPa}$, 2 layers of reinforcement floor $\phi 10$ a 100 (11 $\phi 10$ /1 layer). This beam structure was authored by Cuong Ngo Huu (2006) in his study and used the fiber method and Abaqus program to analyze. Applying the proposed research results (the distributed plasticity deformation method) to nonlinear analysis of beam structure with concentrated plastic hinge and distributed plastic hinge and gave the following results:



Research name	M_p	λ_p	Difference from SPH
SPH	283,7	0,82	
ABAQUS		0,82	0%
SAP2000	282,2		0,53%
Eurocode 4	275,3		2,96%

Figure 4.6. Simple beam subjected to concentrated load **Table 4.1.** comparing values of λ_p and M_p

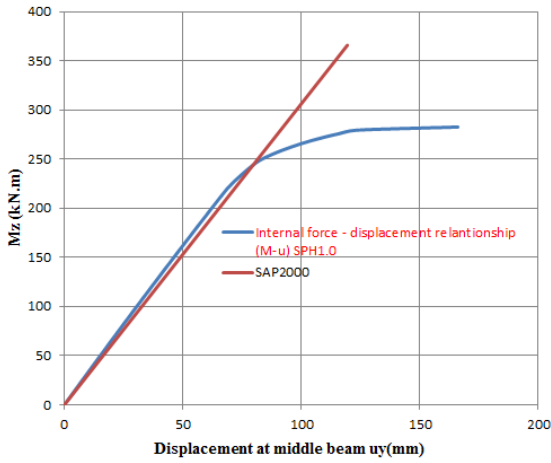


Figure 4.7. Moment-displacement relationship at position middle beams

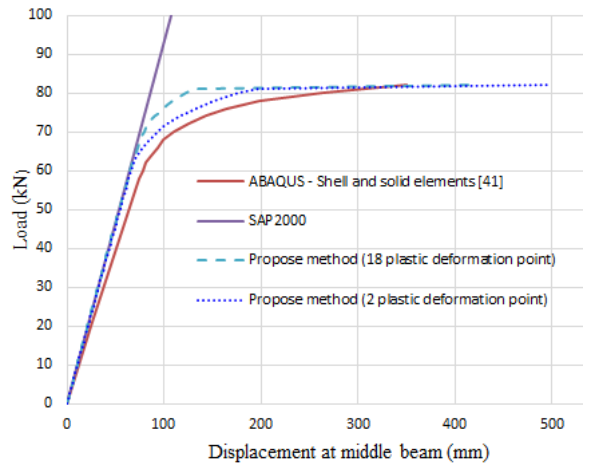
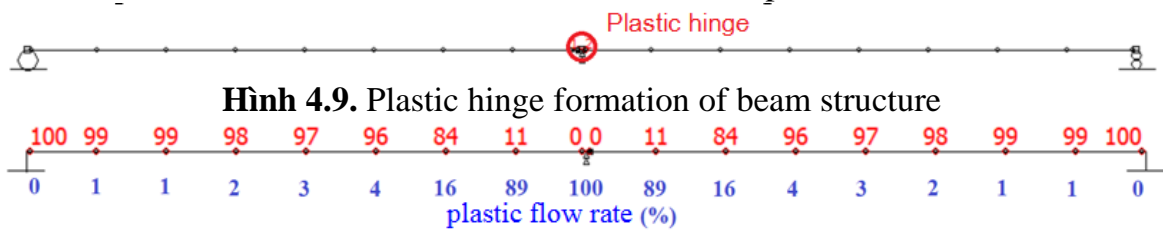


Figure 4.8. Load-displacement relationship at position middle beams



Hình 4.9. Plastic hinge formation of beam structure

Figure 4.10. Stiffness EI_t/EI_{max} and plastic flow rate of the section at plastic failure state
Commenting results::

- From the graphs of figure 4.7 and figure 4.8, it can be clearly seen that when the material is still elastic, the results of the study completely coincide with the results running from the SAP2000 program, when the elastic plastic results are similar to the results previous research, which confirms the reliability of the research method, also shows that the load-displacement relationship is nonlinear, from elastic, elastic plastic and fully plastic, can be determined internally force of composite beam.

- The results of the study were compared with the results of the author Cuong Ngo Huu (2006) showing that the displacement load relationship curve are similar and approximately identical (figure 4.8). From table 4.1: coefficient of limited load λ_p of research method and coefficient λ_p when analyzed by Abaqus and Cuong Ngo Huu (2006) coincide. The value of λ_p of the problem = 0.82 < 1 shows that when the applied load $P = 82T$, the system will be failed, the section of the middle span can no longer bear the strength and form plastic hinge.

- From table 4.1: Research results of M_p value calculated by SPH are different from those of M_p calculated according to Eurocode 4 and M_p value calculated from SAP2000 is small (difference from 0,5 ÷ 3%) → shows the reliability of the research method.

- From the graph in Figure 4.8 shows that when using distributed plasticity method (18 points of plastic deformation), it is found that when the structure is plastic, with the same load level for smaller displacement than the displacement of the concentrated plastic hinge method (2 points of plastic deformation). This shows that when using a multi-point plastic element, the beam structure is better than that of conventional elements.

- From the graphs of figure 4.9, 4.10 shows the plastic hinge forming order, EI_t/EI_{max} stiffness and plastic flow rate (%) of beam section in plastic collapse state ($\lambda_p=0,82$), section middle beam to plastic flow 100%, sections adjacent to plastic flow edge 89%, 16% Through the value of plastic flow rate, it is possible to evaluate the reserve of bearing capacity of each section in beam structure, which is a new point when using multi-point plastic elements in the proposed distributed plastic deformation method.

4.4.2. Composite steel – concrete continuous beam

Investigation of continuous beams tested by Ansourian (1981) with two samples of CTB1 and CTB2 beams. Section beam includes IPE200 steel girder, 100x800mm concrete slab with CBT1 girder; 100x1300mm with beam CBT2 as shown in Figure 4.11; floor reinforcement using steel $\phi 10$. Compressive strength (tension) of concrete f_c' (f_{ct}) with beams CBT1 = 30 (1,6) Mpa, with beams CBT2 = 50 (3,1) Mpa; ρ concrete = 2.310 kg/m³; elastic modulus of concrete according to Warner et al. 1998 is $E_c = 0.043\rho^{1.5}\sqrt{f_c'} = 26,15.10^3\text{MPa}$, $\epsilon_0 = 0.002$, $\epsilon_u = 0,004$. Yield stress of beam steel $f_y = 277\text{MPa}$; tensile strength of steel floor $f_y = 430\text{MPa}$; elastic modulus of steel $E_s = 2.10^5\text{MPa}$. Force $P = 200\text{kN}$ with beam CBT1; $P = 250\text{kN}$ with CBT2 girder, load step $n_{\text{step}} = P/100$. Applying the proposed research results, using the finite element method with distributed multi-point plastic bar elements (with 22 plastic deformation points) to analyze continuous beam structure and compare with experimental results and the results has been studied.

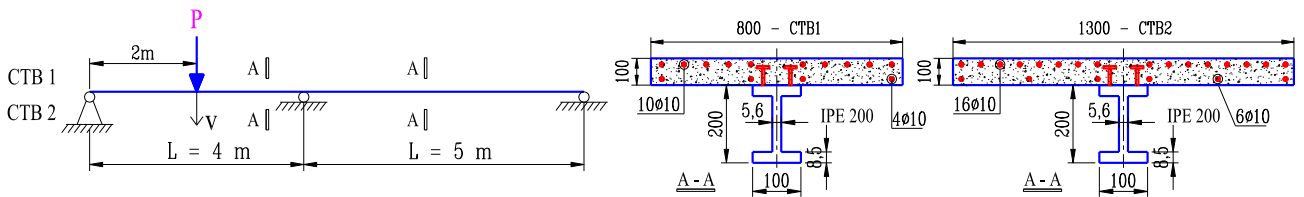


Figure 4.11. 02 samples of CTB1 and CTB2 continuous beams support concentrated load in the middle span

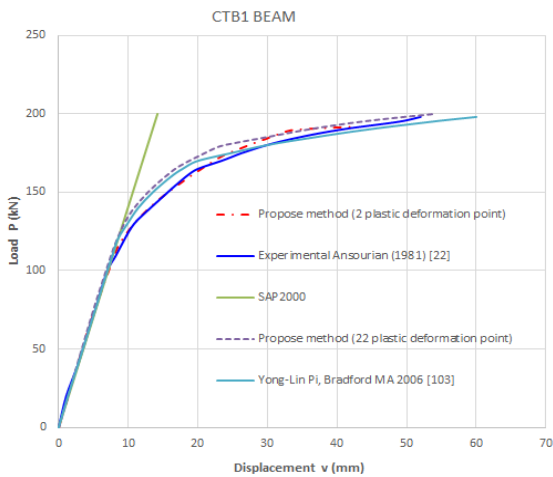


Figure 4.12. Load-displacement relationship at position middle beams CBT1

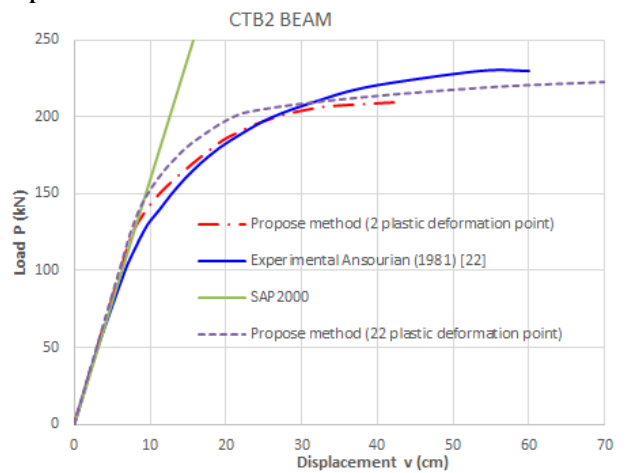


Figure 4.13. Load-displacement relationship at position middle beams CBT2

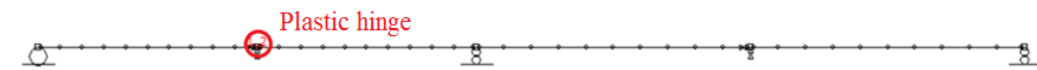


Figure 4.14. Plastic hinge formation of beam structure CBT1

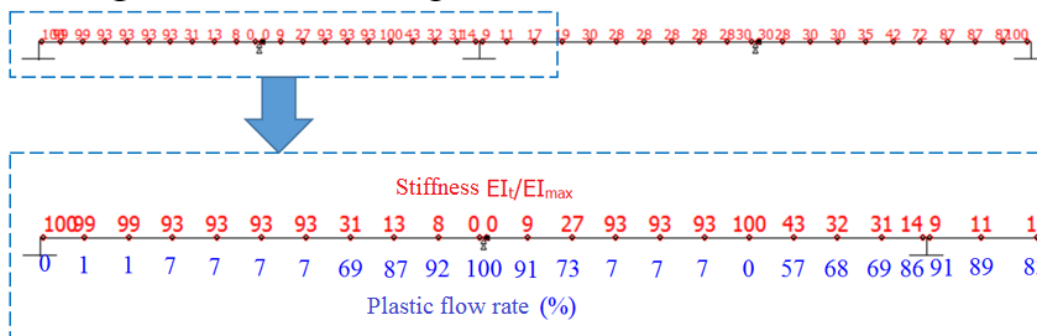


Figure 4.15. Stiffness EI_t/EI_{\max} and plastic flow rate of the section at plastic failure state CBT1

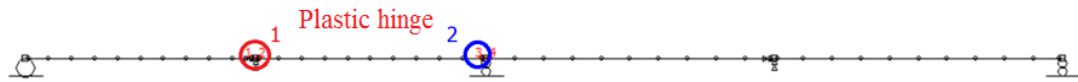


Figure 4.16. Plastic hinge formation of beam structure CBT2

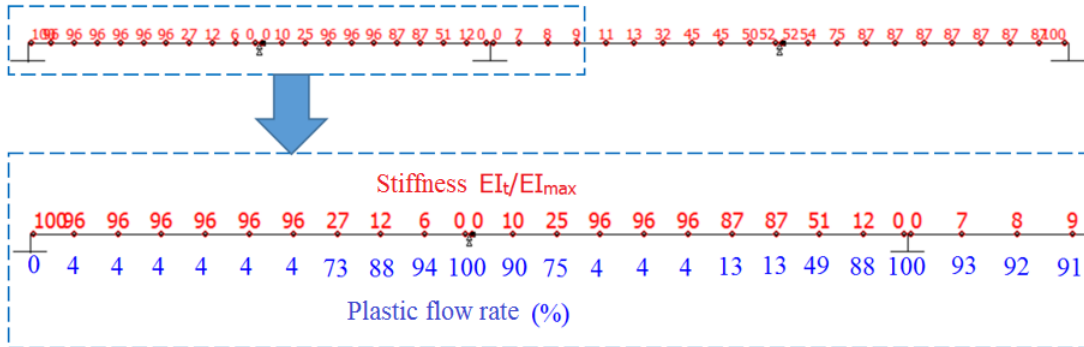


Figure 4.17. Stiffness EI/EI_{max} and plastic flow rate of the section at plastic failure state CBT2

Table 4.2. Table comparing value of M_p of composite continuous beams CTB1, CTB2

Value M_p	CTB1	Comparing of SPH (CBT1)	CTB2	Comparing of SPH (CBT2)
SPH	147,44		158,9	
TN Ansourian (1981)	152	1,8%	164	3,1%
Eurocode 4	137	8,9%	145,8	9,0%

Commenting results::

- From the graphs of figure 4.12 and figure 4.13, it can be clearly seen that when the material is still elastic, the results of the study completely coincide with the results running from the SAP2000 program, When elastic plastic, the results coincide with the experimental results, which confirms the reliability of the research method, also shows that the load-displacement relationship is nonlinear, from elastic, elastic plastic and fully plastic.

- The results of the study were compared with the experimental results by Ansourian (1981) and Bradford MA, Uy B (2006) showing that the displacement - load relationship curve are similar and approximately identical. From Table 4.2 shows that the value of M_p calculated according to SPH compares with the results of M_p according to the Ansourian experiment (1981) and the value of M_p calculated according to Eurocode 4 is not much difference (with the CBT1 beam the different from 1,8% ÷8,9%, with CBT2 girder different from 3,1% ÷9,0%). That shows the reliability of the research method.

- From the graphs of Figure 4.12 and Figure 4.13 shows that when using the method of flexible plastic distribution (22 points of plastic deformation), it is found that when the structure is flexible, with the same load level for smaller displacement than displacement of concentrated plastic hinge (2 points of plastic deformation). This shows that when using a multi-point plastic element, the beam structure is better than that of conventional elements.

- From the graphs of Figure 4.14, 4.16 shows the order of forming plastic hinges, EI/EI_{max} stiffness and plastic flow rate (%) of the beam cross-section in plastic collapse state, the section between the first span of the CBT1 beam flowing 100% plastic, the sections adjacent to the plastic flow 92%, 91% ... the section middle the 1st beat and the pillow of CBT2 beams flowed 100% plastic, the sections adjacent to the plastic flow 90%, 94% ... According to the value of plastic flow rate, it is possible to evaluate the reserve of bearing capacity of each section in beam structure, which is a new point when using multi-point plastic elements in the proposed distributed plastic deformation method.

4.4.3. Composite steel - concrete portal frame with 1 floor and 1 span

Investigation of composite steel-concrete frame with rigid connection at two ends of steel columns, W12x50 steel columns, cross section beam includes W12x27 steel and 102x1219

mm concrete slabs as shown in Figure 4.18 and Table 4.3. The concentrated load is applied $P=150\text{kN}$, loading step $n_{\text{step}}=P/100$. Compressive strength of concrete $f'_c=16\text{MPa}$, $f_{ct}=1,2\text{Mpa}$, elastic modulus of concrete $E_b = 32,5.10^3\text{MPa}$, $\varepsilon_0 = 0.002$, $\varepsilon_u = 0.004$. yield stress of beam steel $f_y = 252,4\text{MPa}$, tensile strength of floor steel $f_y=210\text{MPa}$, elastic modulus of steel $E_s = 2.10^5\text{MPa}$, 2 layers of reinforcement floor $\phi 10\text{a}100$ (11 $\phi 10/1$ layer). Cuong Ngo-Huu, Seung-Eock Kim (2012) used the fiber hinge method and Abaqus to analyze the above structure, with the steel structure modeled by 5852 S4R shell elements, the concrete slabs was modeled by 5376 parts solid C3D8R, analysis time is 48 minutes 20s. C.G Chiorean (2013) used the plastic distribution method using Ramberg-Osgood function to analyze. Applying the proposed research results, using the finite element method with distributed multi-point plastic bar elements with column element using 5 plastic deformation points, beam element using 22 plastic deformation points to analyze Portal frame structure and compare with the results studied.

Table 4.3. Dimensions of section cross-section steel in the Portal frame

Elements	b_f (mm)	t_f (mm)	d (mm)	t_w (mm)
W12x27	165	10,16	304	6,02
W12x50	205,2	16,26	309,6	9,4

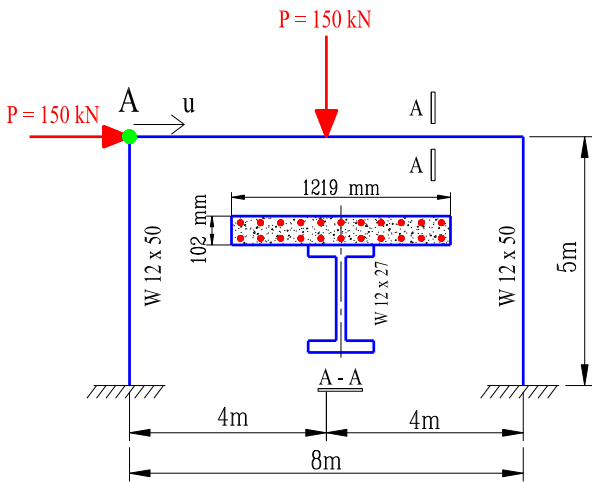


Figure 4.18. Composite Portal frame subjected to concentrated load

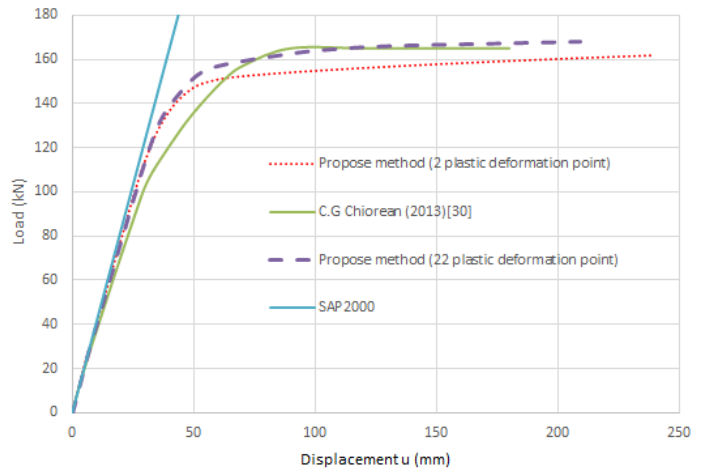


Figure 4.19. Load-horizontal displacement relationship of point A

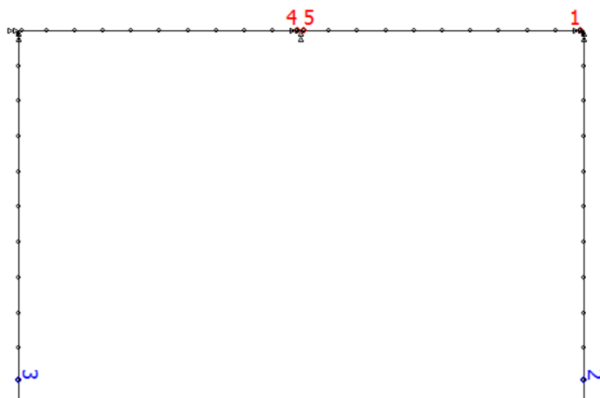


Figure 4.20. Plastic hinge formation of Portal frame

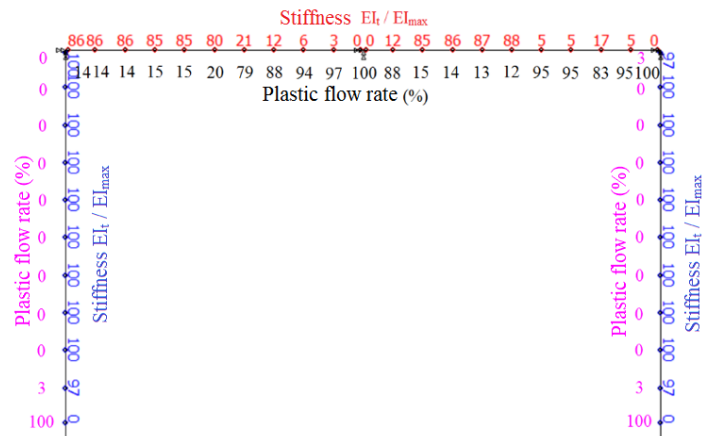


Figure 4.21. Stiffness EI_t/EI_{max} and plastic flow rate of the column, beam section at plastic failure state

Commenting results:

- From the graph in Figure 4.19, it is noticeable that when the material is still elastic, the results of the study completely coincide with the results running from the SAP2000 program, when the elastic plastic the results coincide with the previous research results (CG Chiorean 2013), that confirms the reliability of the research method.

- From the graph of Figure 4.19, it is clear that the load-displacement relationship is nonlinear, from elasticity, elastic plastic and fully plasticity, it is possible to determine the internal force of the composite Portal frame at any step until the frame is damaged.

- From the graph of Figure 4.19, when using distributed plastic hinge method (22 points of plastic deformation), it is found that when the structure is flexible, with the same load level for smaller displacement than the displacement of plastic hinge method (2 points plasticity deformation). This shows that when using multi-point plastic element, the frame structure is better than that of conventional element.

- From the graph of Figure 4.20 shows the order of forming plastic hinges, the first plastic hinge appear at the top of the right beam, the next plastic hinge appear at the foot of the column and finally at the middle of the beam. From the graph in Figure 4.21 shows the EI/EI_{max} stiffness and plastic flow rate (%) of the beam cross-section, the column is in the plastic destructive state, the right beam top section is 100% plastic, the sections adjacent to to the plastic flow 95%, 83% the section middle the beam spans 100%, the sections adjacent to the plastic flow 97%, 88% and plastic flow spread gradually to the side. According to the value of plastic flow rate, it is possible to evaluate the reserve of bearing capacity of each section in beams and columns, which is a new point when using multi-point plastic elements in the proposed distributed plastic deformation method.

- SPH program for short structural analysis time with 2 minutes 40s, it should be said that the equations and solutions are optimal, confirming the advantages of the research method (reducing the calculation volume in analysis process) and it will be very convenient to plastic structure analysis of tall buildings with a large number of elements.

4.4.4. Composite steel - concrete frame with 3 floor and 2 span

Investigation of 3-span 2-span composite steel-concrete frame, structural diagrams conducted by Li, Guo.Qiang and Li, Jin.Jun (2007) with composite steel-concrete beams with rigid connection at 2 ends of steel columns, W12x50 steel columns, cross section beam includes W12x27 steel and 102x1219 mm concrete slabs as shown in Figure 4.22 and table 4.4. The load is concentrated horizontally at the nodes of P (kN), the distributed load is on the beams as shown in Figure 4.23, the loading step is $n_{step} = P/100$ and $n_{step}=q/100$. Compressive strength of concrete $f'_c = 16\text{MPa}$, $f_{ct} = 1,2\text{MPa}$, elastic modulus of concrete $E_c = 0.043\rho^{1.5}\sqrt{f'_c} = 21,5.10^3\text{MPa}$, $\varepsilon_0 = 0.002$, $\varepsilon_u = 0.004$. Yield stress of beam steel $f_y = 252,4\text{MPa}$, elastic modulus of steel $E_s = 2.10^5\text{MPa}$. Li, Guo.Qiang and Li, Jin.Jun used the elastic plastic hinge method to analyze the structure. Applying the proposed research results, using the finite element method with distributed multi-point plastic bar elements to analyze the structure of Li frame with 3 floors and 2 spans and compare with the researched results. Column elements use 5 plastic deformation points, beam elements use 9 plastic deformation points.

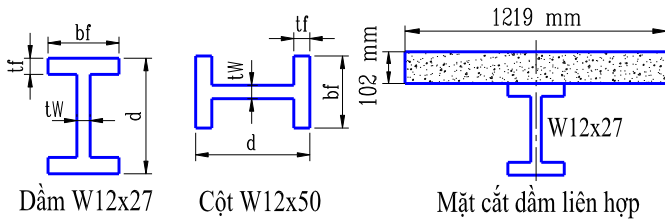


Figure 4.22. Section of beams, steel columns, composite beams in plane frames

Element	b_f (mm)	t_f (mm)	d (mm)	t_w (mm)
W12x27	165	10,16	304	6,02
W12x50	205,2	16,26	309,6	9,4

Table 4.4. Dimensions of section steel in 3 floor frame with 2 spans

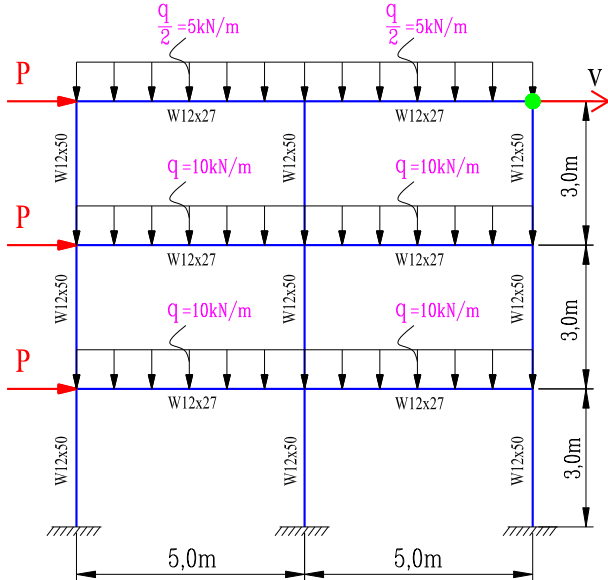


Figure 4.23. Li composite plane frame 3 floors and 2 spans

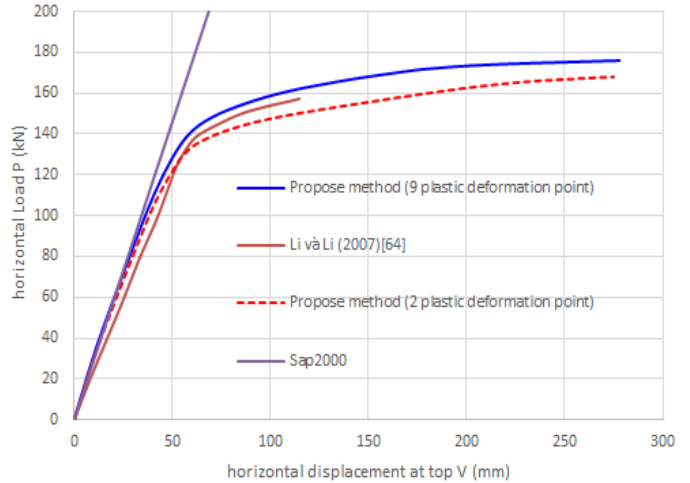


Figure 4.24. Internal force-top displacement relationship of Li frame with 3 spans of 2 spans associated with each load step

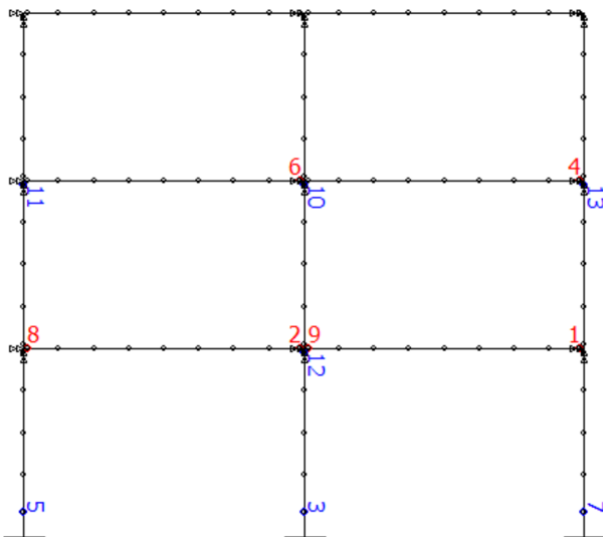


Figure 4.25. Plastic hinge formation of Li frame 3 floors and 2 spans

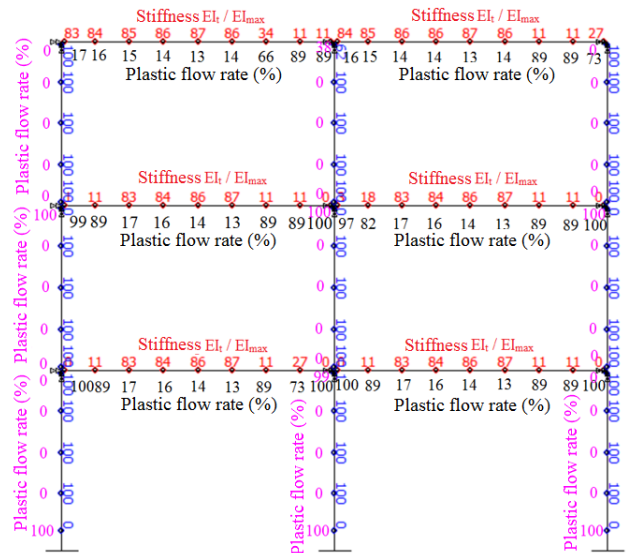


Figure 4.26. Stiffness EI_t/EI_{max} and plastic flow rate of the column, beam section frame at plastic failure state

Commenting results:

- From the graph in Figure 4.24, it can be clearly seen that when the material is still elastic, the results of the study completely coincide with the results running from the SAP2000 program, when the elastic plastic the results coincide with the previous research results (Li and Li), that confirms the reliability of the research method.

- From the graph in Figure 4.24, we can clearly see that the load-displacement relationship is nonlinear, from elasticity, elastic plastic and fully plasticity, we can determine the internal force of the plane frame.

- From the graph in Figure 4.24, when using distributed plastic hinge method, it is found that when the structure is flexible, the same load capacity for displacement is smaller than the displacement of the flexible plastic hinge method (2 points plasticity deformation). This shows that when using multi-point plastic element, the frame structure is better than that of conventional element.

- From the graph in Figure 4.25 showing the order of forming plastic hinge, the first plastic hinge appear at the top of the right beam of the first floor, the next plastic hinge appear when increasing the effective load.

- From the graph in Figure 4.26 shows the stiffness of EI_t/EI_{max} and plastic flow rate (%) of cross section of beams and columns in the state of plastic failure. Through the value of plastic flow rate, it is possible to evaluate the reserve of bearing capacity of each section in beams and columns, which is a new point when using multi-point plastic elements in the proposed distributed plastic deformation method.

- SPH program for short structural analysis time with 4 minutes 15s, it should be said that the equations and solutions are optimal, confirming the advantages of the research method (reducing the calculation volume in analysis process) and it will be very convenient to plastic structure analysis of tall buildings with a large number of elements.

CONCLUSION

NEW RESULTS OF THE THESIS

1. Building the curve ($M-\phi$) relationship of the steel and composite steel-concrete beam to determine the tangent stiffness of these components at different points when the material works in the elastic phase, elastic - plastic and plastic. Establish SPH program to build this relationship.

2. Building the equation of elastic limit surface, intermediate plastic surface, fully plastic surface (failure surface) of the doubly symmetrical wide flange I-section subjected to axial force combined with biaxial bending moments by analytical method and building program to show that surface. The plastic surface depends on the shape of the section and the plastic rotation angle of the section when plastic flow, thus showing the spread plasticity of the steel column cross section during structural analysis. At the same time, based on the plastic surface (interactive surface for bending resistance in two directions), it is possible to test the bearing capacity of the column section, considering that the column section is still in the working state elastic, plastic or has been failed. It has practical significance to evaluate the bearing capacity of the column section corresponding to a certain design load.

3. Building a finite element method and application program for nonlinear analysis of the frame structure with steel column and composite steel-concrete beam considering the plasticity of the material and the spreading plasticity of the structural system. The method has reliability and accurate results compared to the actual working of the structure, significantly reducing the size of the problem of structural analysis, increasing the calculation speed quickly.

DEVELOPMENT ORIENTATIONS OF THE THESIS

1. Continuing to research and develop the plastic and failure surface equations for steel column sections of any shape and composite column section.

2. Building analytical theory for the structural problem of dynamic load.

3. Plastic analysis of the composite structure with concrete-covered columns subjected to static and dynamic loads.

CATEGORY

PUBLISHED ARTICLES OF THE AUTHOR RELATED TO THE THESIS.

1. Hoang Hieu Nghia, Vu Quoc Anh (2013), *To determine the stiffness of semi – rigid connection in composite structures*, Journal of structural engineering and construction Technology, Hanoi, No. 12-2013.
2. Hoang Hieu Nghia (2014), *Composite frame structures – modern structures for Vietnam high rise building*, Journal of science – Hai phong University, No. 7-2014.
3. Hoang Hieu Nghia, Nghiem Manh Hien, Vu Quoc Anh (2014), *Researchs the forming plastic hinge of compressed – bending bars when including effecting of the longitudinal force*, Vietnam Journal of Construction , Hanoi, No. 6-2014.
4. Hoang Hieu Nghia, Nghiem Manh Hien, Vu Quoc Anh (2014), *To create the M- θ curve and fully plastic I sections of beam and column by fiber method*, Vietnam Journal of Construction , Hanoi, No. 8-2014.
5. Hoang Hieu Nghia, Vu Quoc Anh (2014), *Researchs the plastic flow and plastic surface of I steel section including effect of axial force*, Vietnam Institute for Building Science and Technology, Hanoi, No. 4-2014
6. Hoang Hieu Nghia, Vu Quoc Anh (2015), *The influence of connection stiffness to internal forced distribution of composite frame structures*, Vietnam Journal of Construction, Hanoi, No. 2-2015 (Annual scientific conference - Hanoi Irrigation University).
7. Hoang Hieu Nghia, Nghiem Manh Hien, Vu Quoc Anh (2015), *Taking into account the plastic flow of composite beam section by fiber method*, Vietnam Journal of Construction, Hanoi, No. 3-2015 (Conference of 45 years of traditional training - Hanoi Architectural University).
8. Hoang Hieu Nghia, Nghiem Manh Hien, Vu Quoc Anh (2015), *Nonlinear analysis of steel-concrete composite beam under static load*, Vietnam Journal of Construction, Hanoi, No. 11-2015.
9. Hoang Hieu Nghia (2016), *Plastic analysis of beams using simple methods*, Vietnam Journal of Construction, Hanoi, No. 3-2016.
10. Hoang Hieu Nghia, Nghiem Manh Hien, Vu Quoc Anh (2016), *Generation of moment - rotation equation of composite beam cross section taking plastic deformation*, Vietnam Journal of Construction, Hanoi, No. 4-2016.
11. Hoang Hieu Nghia, Nghiem Manh Hien, Vu Quoc Anh (2016), *To create the equation of hardening yield surface of I section steel column under uniaxial load by analytical method*, Volume 2, Collection of the 12th National Science Conference - Deformation Solid Mechanics - Duy Tan University, Da Nang City, August 6-7, 2015.
12. Hoang Hieu Nghia, Nghiem Manh Hien, Vu Quoc Anh (2016), *To create the hardening yield surface of I section steel column under uniaxial load $p-m_x-m_y$* , Vietnam Journal of Construction, Hanoi, No. 8-2016.
13. Hoang Hieu Nghia, Nghiem Manh Hien, Vu Quoc Anh (2016), *Generation of full yield surface equation $\Phi(p, m_y, m_x)$ of I section steel column taking change of the section*, Vietnam Journal of Construction, Hanoi, No. 8-2016.
14. Hoang Hieu Nghia, Nghiem Manh Hien, Vu Quoc Anh (2017), *Phân tích dẻo lan truyền dầm liên hợp thép - bê tông chịu tải trọng tĩnh sử dụng siêu phần tử thanh*, Science Journal

of Architecture & Construction - Hanoi Architectural University, Hanoi. No. 28-2017 (Conference on Materials, Structures and Construction Technology – Hanoi 2017 (MSC 2017)).

15. Hoang Hieu Nghia, Nghiem Manh Hien, Vu Quoc Anh (2018), *The spread of plasticity analysis of steel-concrete composite plane frame static load using super element*, Vietnam Journal of Construction, Hanoi, No. 3-2018.
16. Anh Quoc Vu, Nghia Hieu Hoang, Hien Manh Nghiem (2019), *Distributed Plastic Hinge Method of Composite Steel-Concrete Beams*, Journal of Structures, ISSN 2352-0124 in ISI and SCOPUS journal list) (Reviewing).
17. Anh Quoc Vu, Nghia Hieu Hoang, Hien Manh Nghiem (2020), *Efficient method for yield surfaces of doubly symmetrical sections in nonlinear analysis of steel frame*, the International Journal of Advanced Steel Construction, ISSN 1816-112X (in ISI and SCOPUS journal list) (Reviewing).